Copy No.
RM No. L8H26

NACA RM No. L8H26

Inactive

NACA

RESEARCH MEMORANDUM

FLIGHT INVESTIGATION OF 6.25-INCH-DIAMETER DEACON ROCKET AND 10-INCH-SCALE MODEL ROCKET

By

R. S. Watson

Langley Aeronautical Laboratory
Langley Air Force Base, Va.

NATIONAL ADVISORY COMMITTEE FOR AERONAUTICS

WASHINGTON
March 25, 1949

NACA RM No. L8H26

NATIONAL ADVISORY COMMITTEE FOR AERONAUTICS

RESEARCH MEMORANDUM

FLIGHT INVESTIGATION OF 6.25-INCH-DIAMETER DEACON ROCKET AND 10-INCH-SCALE MODEL ROCKET

By R. S. Watson

SUMMARY

Flight tests were conducted at the NACA Pilotless Aircraft Research Station, Wallops Island, to determine the characteristics of the Allegany Ballistics Laboratory's 6.25-inch-diameter Deacon and 10-inch-scale model solid-propellant rocket motors. The tests were performed to assist in the development of these rockets which were designed for, and urgently needed to propel supersonic research models and pilotless aircraft. The tests showed that the rocket motors functioned properly under various flight-acceleration loads over a range of preignition grain temperatures. A maximum velocity of 4180 feet per second was obtained at an elapsed time of 2.9 seconds with the 6.25-inch Deacon rocket motor at a gross weight of 190 pounds. Free-flight data of drag coefficient for the Deacon configuration for a Mach number range of 1.1 to 3.6 have been obtained from flight tests of several rounds. Camera studies of the take-off and flights of the Deacon rocket showed no evidence of breakup of propellant grains.

An analysis of the forces to which the Deacon rocket grain is subjected was made. The analysis shows that the grain loading is most severe near the beginning and near the end of the rocket action time.

The 10-inch-scale model rocket motor is a scaled model of the 16-inch-diameter multiperforated, cast-grain rocket motor. A maximum velocity of 1625 feet per second at a time of 1.075 seconds was obtained at a gross weight of 309 pounds.

INTRODUCTION

Tests of a solid-propellant rocket on a thrust stand alone are inadequate to demonstrate that the design of the rocket is satisfactory. The thrust stand yields a time history of the thrust developed by the rocket, and the auxiliary equipment normally used in conjunction with the thrust stand gives time histories of the internal pressure. Although these measurements are highly useful in the development of a rocket design, in the thrust stand test the rocket is not subjected to the accelerations which it encounters in flight and which impose additional loads on every component of the rocket. In general, there exists for every rocket a limiting acceleration above which it will not function properly. Many high-performance rockets are capable of achieving this acceleration when propelling a sufficiently light pay load. In solid-propellant rocket design it is frequently found that the component least susceptible to being designed to withstand the acceleration loads is the propellant. Structural failure of the propellant during burning may result in the loss of performance by the ejection of unburned propellant particles through the nozzle, and the resultant exposure of excessive propellant surface to burning may cause abnormal internal pressures leading to erratic thrust and possible rupture of the combustion chamber.

The susceptibility of solid propellants to structural failure under acceleration is influenced by the temperature of the propellant prior to ignition of the rocket. This is due to changes in the mechanical properties, brittleness at low temperatures and excessive plasticity at elevated preignition temperature, and changes in the burning characteristics of the propellant. Proof of the ability of a rocket design to withstand the adverse effects of acceleration can be obtained only by flight tests of the rocket under various conditions of acceleration and initial temperature.

The Pilotless Aircraft Research Division of the NACA, in adapting standard military solid-propellant rockets for use as propulsion units in aerodynamic research models, developed a technique of rapidly measuring the performance characteristics of rockets in free flight. This technique employs a continuous-wave Doppler radar unit which gives, with a minimum of computation, time histories of the displacement, velocity, and acceleration of the rocket. These data, together with standard meteorological sounding data, yield by simple calculations a time history of the rocket thrust, as well as the drag coefficient of the rocket as a function of the Mach number. To fulfill needs of the NACA for rocket motors appropriate for propelling aerodynamic research models to supersonic speeds, this technique has been employed to measure the performance characteristics in free flight of two new high-performance solid-propellant rockets of unconventional design under various conditions of acceleration and preignition temperature of the propellant. The rockets tested were the 6.25-inch-diameter Deacon and a 10-inch-diameter scale model of a 16-inch-diameter, multiperforated, cast-grain rocket. For economy and ease of construction, handling, and testing, the 10-inch-diameter rocket was designed to conduct the research and development for the 16-inch-diameter motor. These rockets were designed and constructed by the Allegany Ballistics Laboratory of the Hercules Powder Company.

Both the Deacon rocket motor and the 16-inch multiperforated cast-grain motors were designed to propel research models. The temperature range tested, 40° F to 120° F, covers the moderate variation in temperature expected in this field of work. Acceleration tests up to 65 times gravity for the Deacon and to 60 times gravity for the scale model covered the range of accelerations anticipated in the use of these motors.

SYMBOLS

a	acceleration, feet per second per second
a_d	deceleration, feet per second per second
C_D	drag coefficient
D	drag, pounds
g	acceleration of gravity, 32.17 feet per second per second
M	mass, slugs (W/g) or Mach number
t	time, seconds
T	thrust, pounds
V	flight velocity, feet per second
W	weight, pounds
θ	flight-path angle, degrees

DESCRIPTION OF ROCKET MOTORS AND TESTING TECHNIQUE

The 6.25-inch-diameter Deacon rocket.- The external configuration and dimensions of the Deacon rocket motor equipped with the head and stabilizing fins used in the flight tests are shown in figure 1(a). The case diameter of the motor was 6.25 inches, but the maximum diameter upon which the drag coefficients have been based was the head diameter of 6.75 inches. The detail dimensions of the nose and tail assembly for the Deacon flight model are shown in figure 1(b). The weights of the various rounds are given in the table in figure 1(a). Variation of the individual round's weight to obtain different accelerations was achieved by changing the mass of the steel heads without altering their maximum diameter or apex angle. Because of the range limitations of the Doppler radar unit, a reduced amount of propellant was employed in the tenth Deacon round listed in the table of figure 1(a) in order to provide measurements of drag at speeds below a Mach number of 2. This round was made by turning down the diameter of the grain until the proper weight reduction of the grain was obtained. Additional restrictor was used to fill the area occupied by the grain which was removed. Therefore, the same external configuration was retained; and since the specific weights of the restrictor and grain are approximately equal, the center-of-gravity location was maintained.

A cross section of the Deacon rocket showing the internal configuration is given in figure 1(c). The propellant grain is a star-perforated cylinder covered with a restricting material on the outside cylindrical surface. Since burning proceeds from the surface of the star perforation outwards toward the case, the propellant and restrictor serve as thermal insulation for the case, thus preventing the waste of energy as loss of heat through the case. This thermal insulation also made possible the construction of the case from a light-weight, high-strength alloy. Due to the length of the rocket it is impractical with standard manufacturing tolerances to obtain a fit such that there is no space between the outside surface of the grain restrictor and the inside surface of the case. Passage of combustion gases, and hence pressure, into this space between the grain and case is prevented by means of an obturating gasket at the forward end of the grain and by a sealing putty at the rear end of the grain. Consequently, upon ignition the pressure within the star perforation expands the grain and restrictor until they seal firmly against the case. The grain is restrained against longitudinal movement due to acceleration and other forces by means of a narrow shoulder at the entrance of the nozzle. The periphery of the grain rests upon this shoulder. Additional support is obtained from the static friction between the grain and the case. This method of grain support minimizes the blocking of the nozzle entrance.

<u>The 10-inch-diameter rocket</u>.- The flight-test external configuration and dimensions of the 10-inch-diameter scale model of the 16-inch-diameter multiperforated, cast-grain rocket is shown in figure 1(d). The external configuration was chosen for ease of construction and alteration of weight to achieve different accelerations rather than for excellence of aerodynamic properties. The construction details of the nose and tail assembly of the flight version of the 10-inch-scale rocket motor are shown in figure 1(e). The different weights are achieved by lightening the head without altering the external shape of the rocket. The weights of the eight rounds tested are given in the table of figure 1(d).

The 10-inch-scale model rocket motor used the 8.43-inch-diameter multiperforated, cast-grain propellant. A cross section of the rocket grain is shown in figure 1(f). The grain was restrained against longitudinal movement due to acceleration and other forces by a narrow shoulder at the nozzle entrance upon which the periphery of the grain rested. The acceleration and other loads upon the central parts of the grain were therefore transmitted through the propellant to this shoulder.

Test conditions.— Five of the 6.25-inch-diameter Deacon rockets, rounds one to five, inclusive, of figure 1(a), were tested at a preignition temperature of 77° F, each at a progressively greater acceleration effected by reducing the head weight. Upon completion of these firings with no evidence of malfunctioning, tests were made at elevated and reduced preignition temperatures by firing four more rounds at weights approximately equal to the minimum weight of the 77° F firings. Two of these rounds, numbers 6 and 7, were fired at a preignition temperature of 120° F, and two, numbers 8 and 9, were at a preignition temperature of 40° F. Round number 10, which was for the purpose of obtaining drag measurements at speeds below a Mach number of two, was fired at a preignition temperature of 77° F.

The 100-watt CW Doppler radar is capable of obtaining velocity data for the Deacon configuration up to ranges of 20,000 feet. It was found that the coasting velocity of a nominal Deacon at this range was in excess of Mach number 2. By reducing the propellant and thereby decreasing the burning time, the range and velocity at burnout would be lower, and therefore a lower velocity range can be investigated before the round's flight range exceeds 20,000 feet. Consequently, round number 10 was fired with a propellant weight designed to give a maximum velocity equal to the velocity of the full charge rounds at a range of 20,000 feet.

Three of the 10-inch-diameter scale model cast-grain rockets, rounds numbers one to three, inclusive, of figure 1(d), were fired at a 77° F preignition temperature but at different weights in order to obtain different accelerations. Upon completion of these firings without evidence of malfunctioning, five additional rounds were fired at elevated and lowered preignition temperatures, all at approximately the same weight, but a weight which was less than the minimum weight of the 77° F firings (fig. 1(d)). The elevated temperature rounds, numbers 4, 5, and 6, were fired at a preignition temperature of 120° F; and the reduced temperature rounds, numbers 7 and 8, at 40° F.

The rockets were brought to the desired preignition temperature by conditioning in a temperature-controlled chamber for a length of time sufficient for attainment of uniform temperature throughout the propellant. They were then flight-tested immediately after removal from the conditioning chamber in order to insure no appreciable change in temperature.

Test technique.— All of the rockets were launched from the ground at an elevation angle of 70° in order that the early part of their trajectories, during which the radar velocity measurements were made, would be approximately straight lines. Time histories of the rocket velocity during approximately the latter two-thirds of the thrusting time in the case of the Deacon rockets, and approximately the latter half of the thrusting time in the case of the 10-inch-scale model rockets, were obtained by a 100-watt continuous-wave Doppler radar. In addition, this unit gave for both rockets the flight velocity subsequent to burnout for a considerable length of time.

The radar unit was located as closely adjacent to the point of launching as was practical with the beam pointing along the trajectory. It measures the velocity of recession of an object by means of the Doppler effect. This system has been described in reference 1. The Doppler radar data also yield the slant ranges of the rockets, from which the altitudes can be determined by assuming straight-line trajectories. Measurements of velocity by means of the Doppler radar during the initial flight of the rockets were precluded by inability to track with the radar equipment. Adequate protection of the radar and its tracking crew required placing the equipment 150 feet from the launcher. For the first fraction of a second of the flight no radar data could be taken. The short burning time of the 10-inch-scale model rocket motor prevented the taking of radar data for most of the burning period, and the tests of these rocket motors were conducted without attempting to obtain the thrust time histories.

Fixed-line-of-sight, high-speed, 35-millimeter motion-picture cameras were located so as to cover the launching and the first 100 feet of the trajectory of the Deacon rockets, and the launching and the first 1000 feet of the trajectory of the 10-inch-diameter rockets. The cameras provided measurements of the time delay between ignition and the beginning of motion, time histories of the initial part of the trajectories, and qualitative information on the ignition and build up of thrust as evidenced by the jet exhaust and flame patterns.

The records from all instruments were time-synchronized by means of a master electric timer.

At the time of the tests, measurements of the pressure and temperature of the atmosphere were made by standard radiosondes. From these measurements, the velocity of sound and the density as a function of geometric altitude can be computed.

<u>Accuracies</u>.- Radar velocity measurements have been previously compared with other methods of velocity measurements and have been found to agree within 1 percent (reference 1). From SCR-584 tracking data for round 8 at an elapsed time of 14 seconds, the error due to curvature of the flight path was less than 1 percent, and for round 10, less than 1 percent at 11 seconds. The camera data were less accurate than the radar data and were used only where radar data were not obtainable. Time measurements are electronically controlled to 0.01 percent and the instant of firing may be in error by 0.005 second.

Experience has shown that the mean curve of the drag data of five rounds reduced from Doppler radar records may be expected to be within 1 percent of the mean curve of 95 percent of the rounds (reference 2). Loss of any grain-restricting material during burning would result in an additional error in the calculated drag.

The assumption of the mass being burned at a constant rate results in an error of less than 2 percent of the thrust. Because of the decrease in atmospheric pressure at altitude, the thrust measured at altitude is greater than the thrust at sea level by an amount equal to the product of the exit area of the nozzle and the difference in pressure at sea level and altitude.

RESULTS AND DISCUSSION

The 6.25-Inch-Diameter Deacon Rocket

Velocity.- Time histories of the velocity of Deacon rounds, numbers 2 to 10, inclusive, are given in figure 2. No data were obtained from round number 1 because of instrument failures. The solid-line portion of the velocity curves was obtained from the Doppler radar. The initial part of the velocity curve that is shown as a broken line was obtained from the camera data and interpolation between the radar and camera data. Zero time in figure 2 and in all other figures corresponds to the instant of application of the firing voltage. The velocity time curves show that a time delay occurred between the application of firing voltage and the beginning of motion of the rocket. The maximum velocity and its instant of occurrence are given in the figures.

Round number 6 achieved a maximum velocity of 4180 feet per second at an elapsed time of 2.9 seconds at a gross weight of 190 pounds.

Acceleration.- Time histories of the acceleration of the Deacon rockets are presented in figure 3. These curves were obtained by differentiation of the time histories of the velocity. The solid and broken portions of the curves correspond to the similar parts of the curves of velocity given in figure 2. It can be seen that, within the range of preignition temperatures and gross weights investigated, the maximum acceleration consistently occurred shortly before burnout of the rocket.

A maximum acceleration of 66 times gravity was reached by round number 5 at 2.6 seconds.

Drag coefficient.- The drag of the rocket during the coasting period is equal to the product of the deceleration and the mass of the rocket at burnout diminished by the component of the weight in the direction of the flight path as given by the equation of motion $D = Ma_d - W \sin \theta$. The assumption was made that the mass of the rocket at burnout and during the coasting period of the flight is equal to the initial mass of the metal parts plus the initial mass of the restricting material. Utilizing the radiosonde data and the flight trajectories, the drag was converted to a drag coefficient based on the maximum diameter of the rockets, which was 6.75 inches. This coefficient is shown plotted against flight Mach number in figure 4 for the Deacon rockets. In the technique used, the range of the CW Doppler radar limited the drag data for the lower Mach numbers, and even considering the reduced velocity of the special round 10, the drag data were for speeds in excess of Mach number 1. Therefore, the curve of drag coefficient does not extend below Mach number 1.1. The drag-coefficient data shown in figure 4 show good agreement between Mach numbers of 2.0 and 3.6 for the various rounds tested. As shown in figure 4, the variation of drag coefficient with Mach number for the Deacon configuration can be approximated by an expression of the type $\left(\frac{1 + \frac{1}{\sqrt{M^2 - 1}}}{2}\right)$.

Thrust.- The thrust of the rocket at any instant is equal to the sum of the product of the total mass and acceleration, the drag, and the component of weight in the direction of the flight path as given by the following equation of motion:

$$T = Ma + D + W \sin \theta$$

The instantaneous mass of the rocket was taken as the initial mass of the rocket less the mass of propellant expended. The propellant was assumed to be expended at a constant rate throughout the burning period. The values of acceleration were taken from figure 3.

The time histories of the drag during the burning period were computed from the curve of drag coefficient in figure 4, the radar velocity, and atmospheric data. The drag-coefficient data of figure 4 were corrected for base pressure drag over the nozzle area during coasting using data reported in reference 3. No data for drag below a Mach number of 1 were available. Since the drag in this region is a small fraction of the thrust, it could be neglected. However the subsonic drag was assumed to be given by the dotted curve of figure 5. θ is again assumed constant. The thrust and the various items of the equation of motion are shown in figure 5. The broken portions of the curves Ma and thrust in figure 5 correspond to similar portions of the acceleration curves (fig. 3).

It will be noted that there are two thrust peaks shown in figure 5, one near the beginning and one near the end of the burning period. The small port area of the propellant creates a significant degree of erosion of the rear portion of the propellant grain during the early part of the burning period. The first thrust peak is a result of the increase in burning rate due to the erosive action of the high-velocity gases passing through the restricted port area. As burning progresses the increase in port area reduces the erosion and the thrust reaches a minimum. Throughout the burning period the burning surface increases. The burning surface and burning rate finally increase sufficiently to create the second thrust peak.

Figure 5(b) shows that round 3 has some fluctuation in thrust during the first second of burning.

The values of the total impulse of the Deacon rounds are equal to the areas over the thrust-time curves of figure 5. The values of total impulse are given in table 1. The variation of the individual rounds is within 4 percent of the average value of 19,680 pound-seconds. The average value compares closely with the design value of 20,000 pound-seconds (reference 4).

<u>Forces acting on propellant grain</u>.– In the static tests of rocket motors, there are two forces tending to dislodge the grain in the longitudinal direction; namely, the force due to the difference in the gas pressures acting on the two ends of the grain and the viscous friction force of the flow of gases along the grain. In flight these same forces are present as well as an additional force due to the inertia of the grain. To show the magnitude of the forces acting on the propellant grain, the pressure, viscous, and inertia forces were calculated for round number 5. Computations of the pressure and friction forces were made by the methods of reference 5. The inertia force acting on the propellant grain was the product of the grain mass and instantaneous value of acceleration obtained from figure 3(d). The time histories are presented in figure 6. The variations of the viscous and pressure forces are similar. These forces reach a maximum within a half second after firing and drop off rapidly until burnout. The acceleration load reaches its peak slightly later and decreases only gradually until just before burnout. Figure 6 also shows the total force acting on the propellant grain in flight. For comparison the total force acting on the grain during a ground firing is also given. In both cases the maximum value of the total force reaches a maximum within a short time after firing. These forces have significance if the retaining loads on the propellant grain are critical.

The total grain force was divided by the instantaneous weight to show the average load applied to each unit of grain weight. Plots of this parameter are shown in figure 6(b) both for flight and static firings. The unit loading in static firings has a single maximum coincident with the first thrust peak. However, in flight the average force on each unit of grain weight has a peak about the time of the first thrust peak and another of equal magnitude very close to burnout. Breakup of the grain would therefore be expected near the beginning or near the end of the burning period, if it is to occur.

Effects of preignition temperature.- The initial temperature of the propellant grain affects the internal ballistics of a rocket motor. The burning rate of the grain increases with increasing preignition temperature and leads to higher combustion pressures. Conversely, low preignition temperatures lead to slower burning rates. At extremely low temperatures a violent fluctuation of the burning rate, a phenomenon known as chuffing, is encountered. An additional low-temperature limitation of a rocket motor is the fact that propellant grains become brittle at lowered temperatures with a tendency to crack when stressed by firing pressure or acceleration loads. The cracking of a rocket propellant grain may result in the loss of performance through the loss of propellant or in the destruction of the rocket through an excessive increase in the combustion pressure. An additional possibility is present in the case of the Deacon because of the use of the light alloy case. If cracking of the grain were to expose the case to the flame, failure would occur due to the inability of the case material to withstand high temperatures.

In the present investigation two Deacon motors were fired at a preignition temperature of 40° F, two at 120° F, and six at 77° F, and no motor failures occurred. The range of temperatures covered is great enough to prove the performance of the Deacon for ordinary use. Table I shows only a small variation in total impulse over the range of preignition temperatures. This indicates that no significant amount of propellant was lost due to grain cracking or any other cause. The effect of preignition temperatures on the action time presented in figure 7 is greater at low temperature than over the higher end of the range tested.

Camera studies of launchings.- It had been noted that large forces tended to dislodge the propellant at approximately one-half second after ignition took place. Sequence photographs were taken of the launching and of the first half second of flight. The photographs of round number 1, which are representative of all the launchings, are presented in figure 8. The time at which a photograph was taken is listed opposite each frame. Zero time was taken to be the instant when the electrical voltage was applied to the rocket motor.

A study of the photographs did not reveal any indications that propellant failure occurred, resulting in chunks of propellant in the exhaust jet. Intermittent puffs of black smoke can be observed in the exhaust jet. Occasionally the smoke puffs burst into flame.

The photographs provided a method of determining the ignition delay. From a summary of the data taken from these sequence photographs, it was determined that the ignition delay amounted to 0.025 second. From the instant of ignition, there was an additional delay which averaged 0.055 second before the build up of pressure and thrust resulted in actual motion of the round.

The 10-Inch-Scale Model Cast-Grain Rocket

Velocity.- Time histories of the velocity of the 10-inch-diameter scale model rounds, numbers 1 to 8, inclusive, are given in figure 9. These curves were obtained from CW Doppler radar and camera data in a similar manner as the velocity time curves for the Deacon rounds; however, the camera data for these rounds overlapped the radar data. The short burning time of these rockets in combination with the lower acceleration precluded the use of radar measurements for a large portion of the action time. The radar data did yield the time and the value of the maximum velocity. The values for each are noted in figure 9. A maximum velocity of 1625 feet per second was reached by round number 5 at a time of 1.075 seconds at a gross weight of 309 pounds. This round also had the maximum acceleration of 60.8 times gravity at 0.8 second. The total impulse is given in table II. The variation of the individual rounds is within 4 percent of the average value of 14,070 pound-seconds. This average value is slightly above the design value of 13,900 pound-seconds (reference 4).

Drag coefficient.- Data from the last five rounds give the variation of drag coefficient throughout the transonic range (fig. 10). The drag coefficient is based on the area at the maximum diameter of 11.25 inches.

Effects of preignition temperature.- From the velocity time histories for the 10-inch-diameter rockets (fig. 9), it is possible to approximate closely the values of the action time for the various rounds. The curve of action time as a function of initial temperature presented in figure 11 shows the effects of preignition temperature for the 10-inch-diameter rounds. It can be seen from the uniformity of the action time of the rounds for their respective temperatures that the performance of the rocket motor was satisfactory.

CONCLUSIONS

A flight investigation of the 6.25-inch Deacon rocket motor showed the following:

1. With initial temperature of the grain at 77° F the rocket motor functioned satisfactorily through a range of accelerations up to 66g.

2. With the acceleration limited to approximately 66g the rocket motor functioned satisfactorily at initial temperature limits of 40° F and 120° F.

A flight investigation of the 10-inch-diameter scaled model of the 16-inch-diameter multiperforated, cast-grain rocket motor showed the following:

1. With initial temperature of the grain at 77° F the rocket motor functioned satisfactorily through a range of accelerations up to 60g.

2. With the acceleration limited to approximately 60g the rocket motor functioned satisfactorily at initial temperature limits of 40° F and 120° F.

Langley Aeronautical Laboratory
National Advisory Committee for Aeronautics
Langley Air Force Base, Va.

REFERENCES

1. Pitkin, Marvin, Gardner, William N., and Curfman, Howard J., Jr.: Results of Preliminary Flight Investigation of Aerodynamic Characteristics of the NACA Two-Stage Supersonic Research Model RM-1 Stabilized in Roll at Transonic and Supersonic Velocities. NACA RM No. L6J23, 1946.

2. Katz, Ellis R.: Results of Flight Tests at Supersonic Speeds to Determine the Effect of Body Nose Fineness Ratio on Body and Wing Drag. NACA RM No. L7B19, 1947.

3. Anon.: Survey of Bumblebee Activities. Bumblebee Rep. No. 70, The Johns Hopkins Univ., Appl. Phys. Lab., Nov. 1947.

4. Anon.: Manual of Booster Rockets. RPIA/MI, The Johns Hopkins Univ., Appl. Phys. Lab., Aug. 1, 1947.

5. Anon.: Rocket Fundamentals. OSRD No. 3992, ABL-SR4, NDRC, Div. 3, Sec. H, 1944.

TABLE I

TOTAL IMPULSE OF DEACON

Round number	Initial weight (lb)	Maximum velocity (ft/sec)	Total impulse (lb-sec)	Variation of total impulse (percent)
2	232.65	3307	20008	1.7
3	215.30	3571	19800	.6
4	213.40	3747	20168	2.5
5	197.45	4094	19912	1.2
6	190.50	4180	19512	-.9
7	196.51	4122	19904	1.1
8	196.08	3817	19160	-2.6
9	197.49	3667	18976	-3.6
			av. 19680	

NACA

TABLE II

TOTAL IMPULSE OF 10-INCH-DIAMETER CAST-GRAIN ROCKET

Round number	Initial weight (lb)	Maximum velocity (ft/sec)	Total impulse (lb-sec)	Variation of total impulse (percent)
1	334.58	1430	13860	-1.5
2	339.37	1399	13680	-2.8
3	394.85	1228	14200	.9
4	310.07	1621	14680	4.3
5	308.58	1624	14460	2.8
6	305.07	1619	14140	.5
7	307.64	1523	13850	-1.6
8	316.08	1473	13680	-2.8

NACA

[redacted]

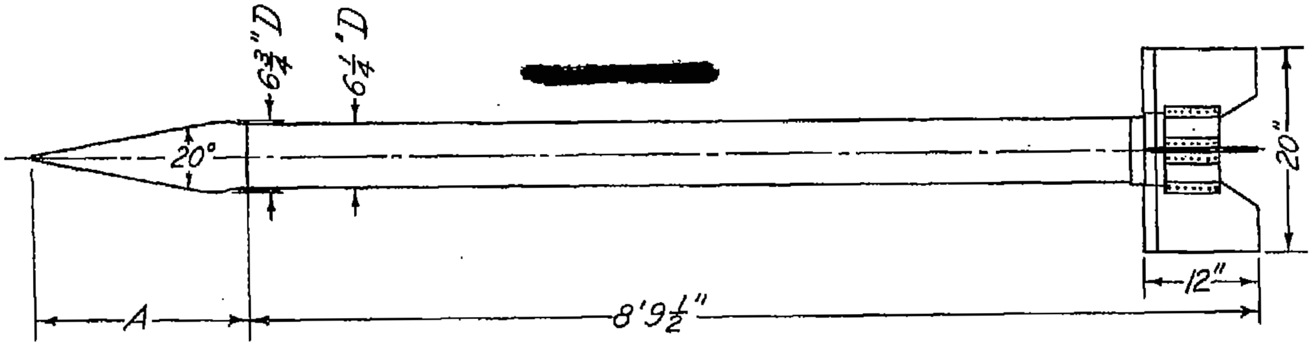

Round number	A, in.	Metal parts weight, lb	Powder weight, lb	Total weight, lb	Preignition Grain Temp., °F
1	23 7/8	142.35	103.2	245.55	77
2	22 3/8	129.55	103.1	232.65	77
3	22 9/16	113.50	101.8	215.30	77
4	22 9/16	110.80	102.6	213.40	77
5	22 9/16	96.25	101.2	197.45	77
6	22 9/16	89.50	101.0	190.50	120
7	22 9/16	95.31	101.2	196.51	120
8	22 9/16	93.26	102.8	196.08	40
9	22 9/16	96.69	100.8	197.49	40
10	22 9/16	132.81	62.3	195.11	77

(a) External configuration of 6.25-inch Deacon rocket motors.

[redacted]

Figure 1.- Configurations of test rounds.

[redacted]

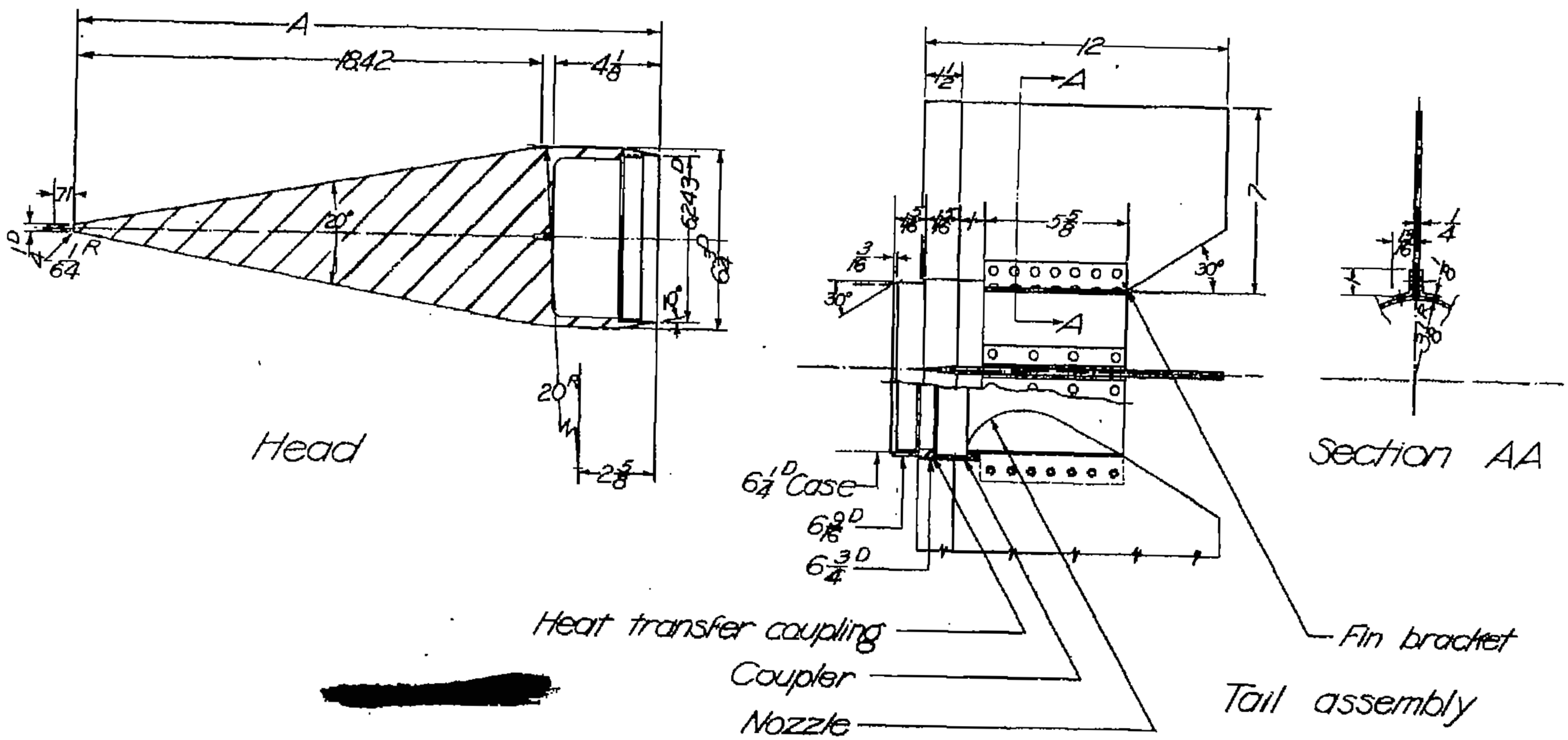

[redacted]

b) Details of 625-inch Deacon rocket motor.
Figure 1.- Continued.

[redacted]

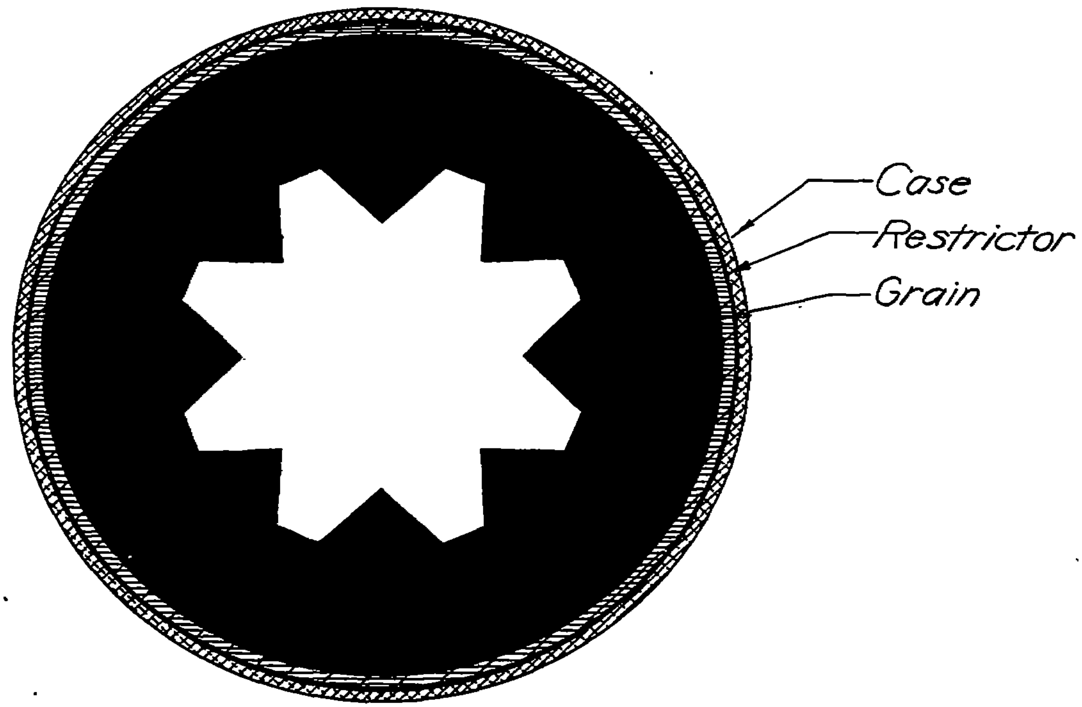

(c) Cross section of 6.25-inch Deacon rocket motor.

[redacted]

Figure 1 - Continued.

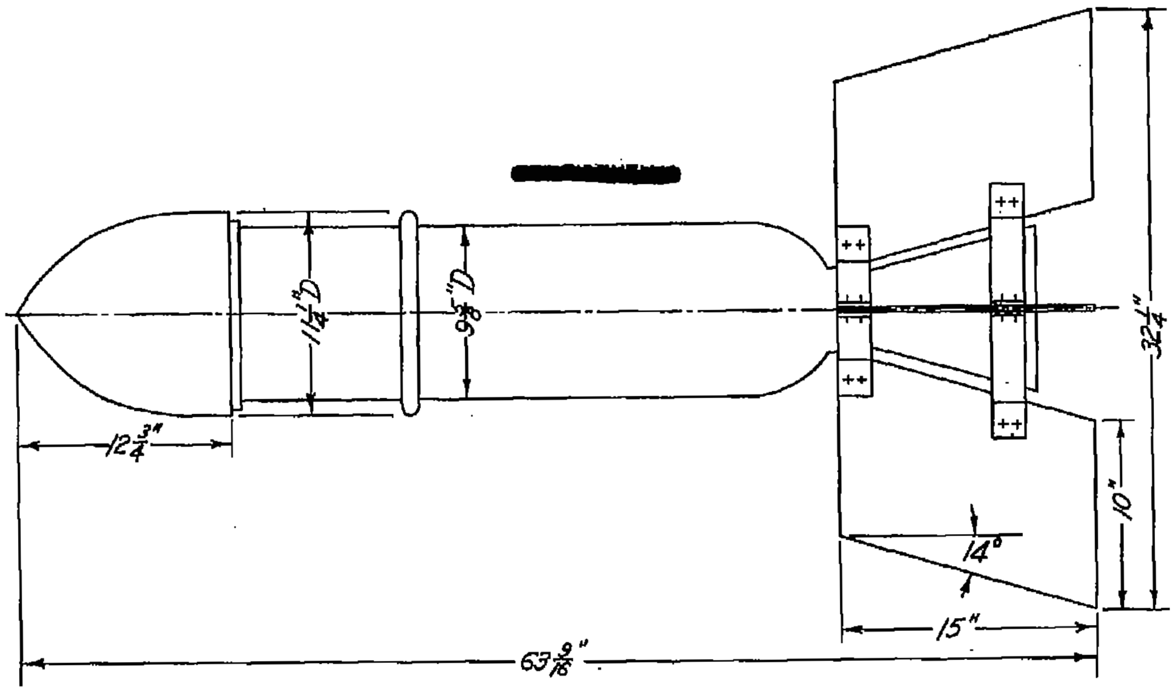

Round number	Metal parts weight, lb	Powder weight, lb	Total weight, lb	Preignition grain temp, °F
1	261.41	73.17	334.58	77
2	265.20	74.17	339.37	77
3	321.05	73.80	394.85	77
4	235.82	74.25	310.07	120
5	235.34	73.22	308.56	120
6	231.10	73.97	305.07	120
7	233.21	74.43	307.64	40
8	241.57	74.51	316.08	40

(d) External configuration of 10-inch-scale model rocket motor.

Figure 1.-Continued. [redacted]

[redacted]

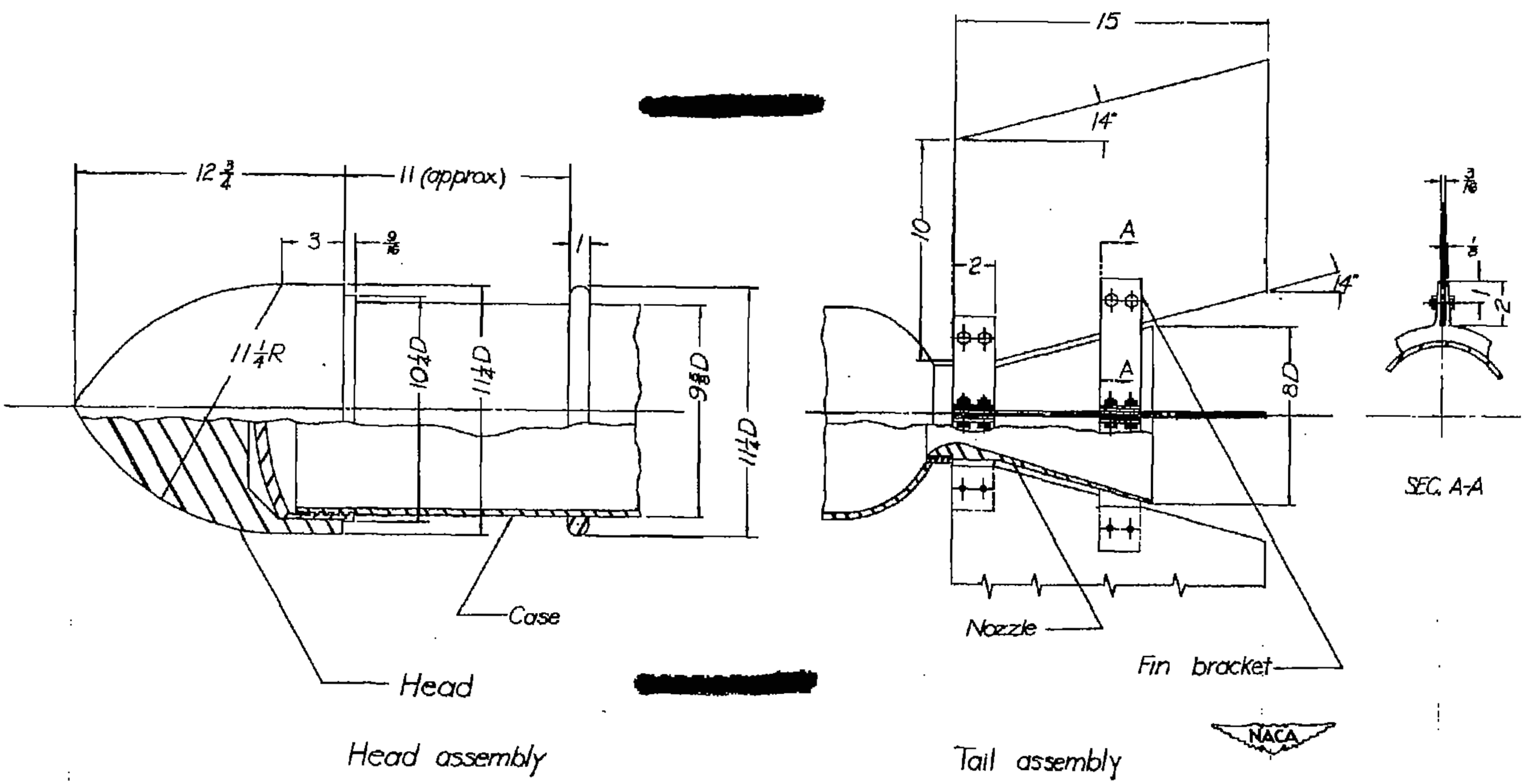

[redacted]

Head assembly

Tail assembly

(e) Details of 10-inch-scale model rocket motor.

Figure 1. - Continued.

[redacted]

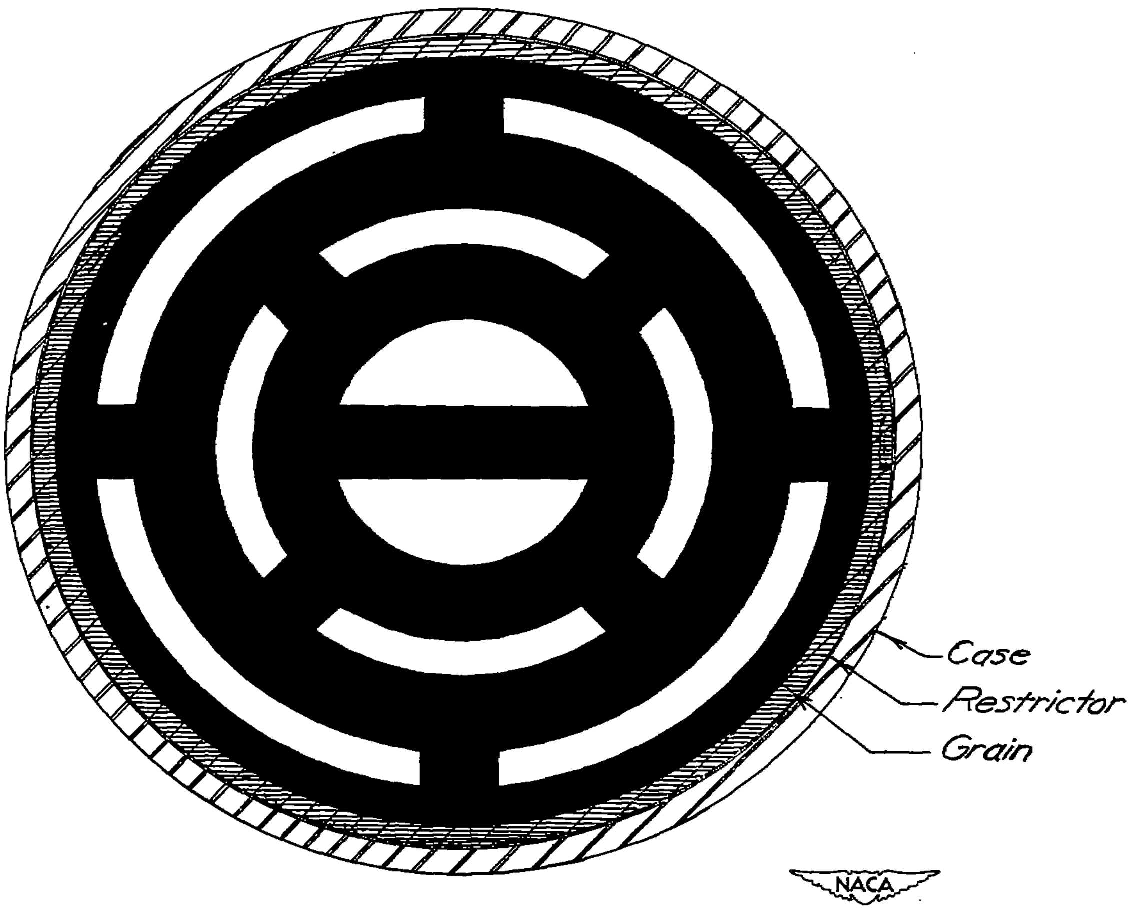

[redacted]

(f) Cross section of 10-inch-scale model rocket motor.

Figure 1.-Concluded.

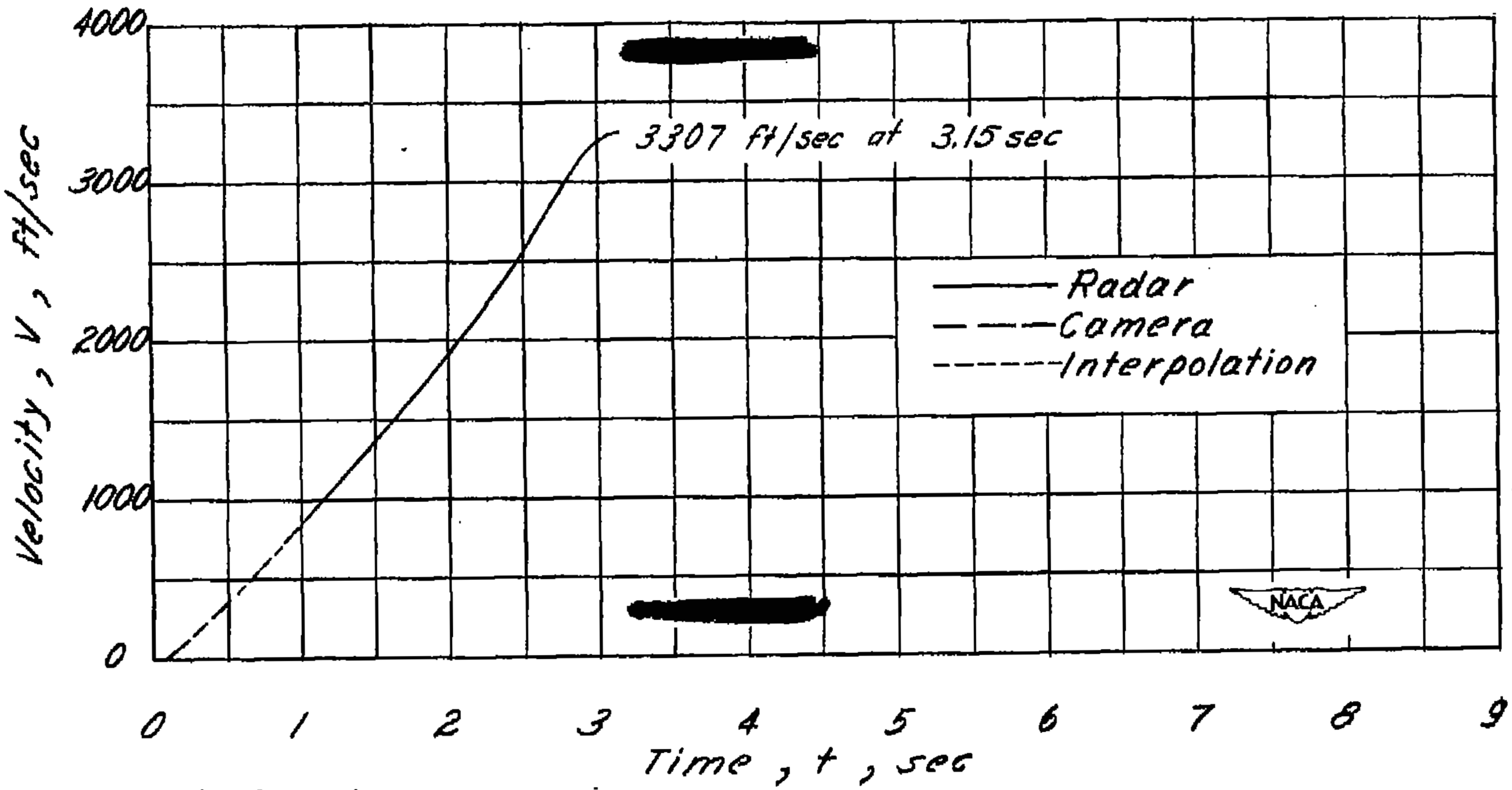

(a) Round 2.

Figure 2.- Velocity-time curves, 6.25-inch Deacon rocket motor.

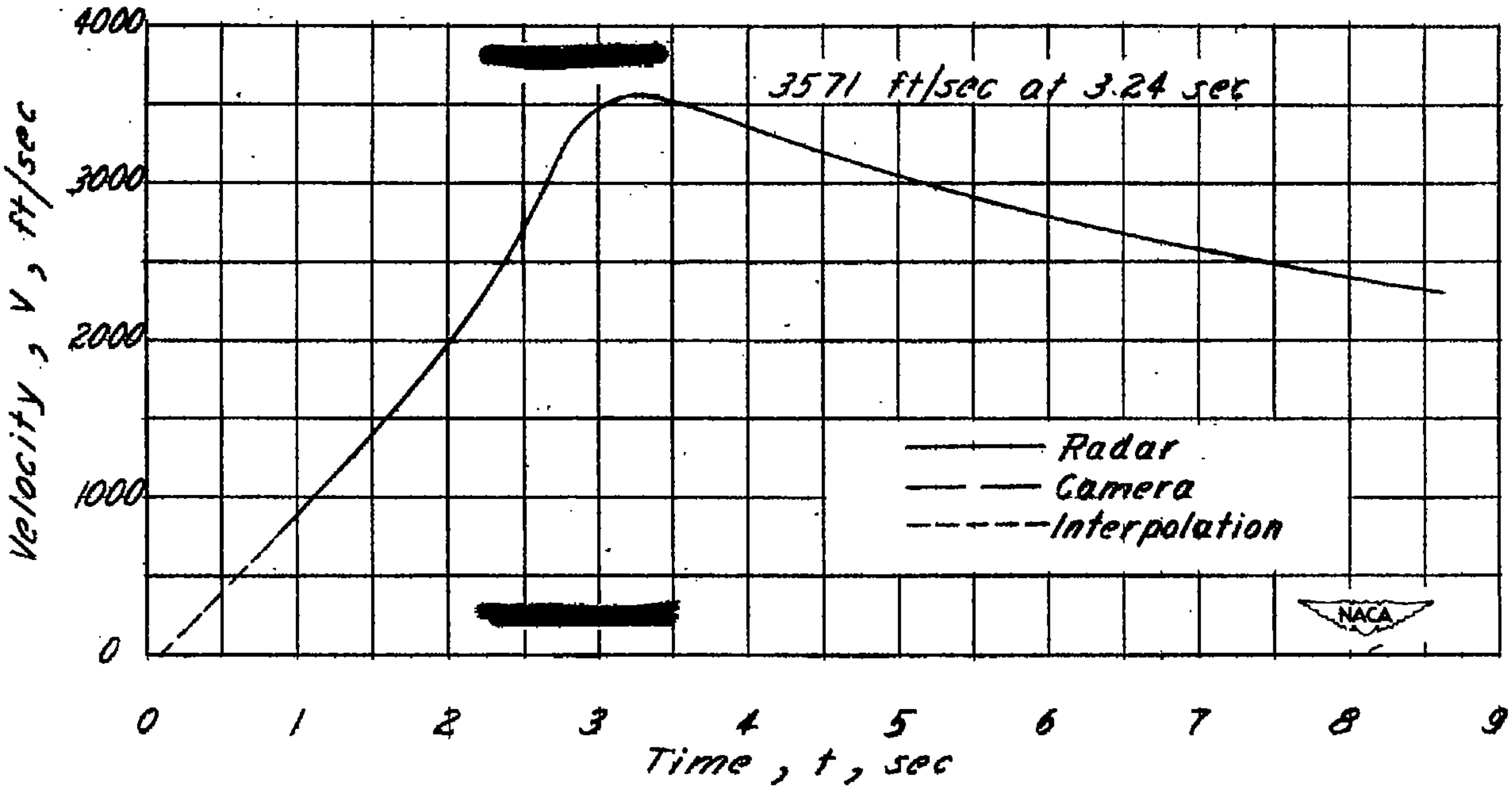

(b) Round 3.
Figure 2.- Continued.

[redacted]

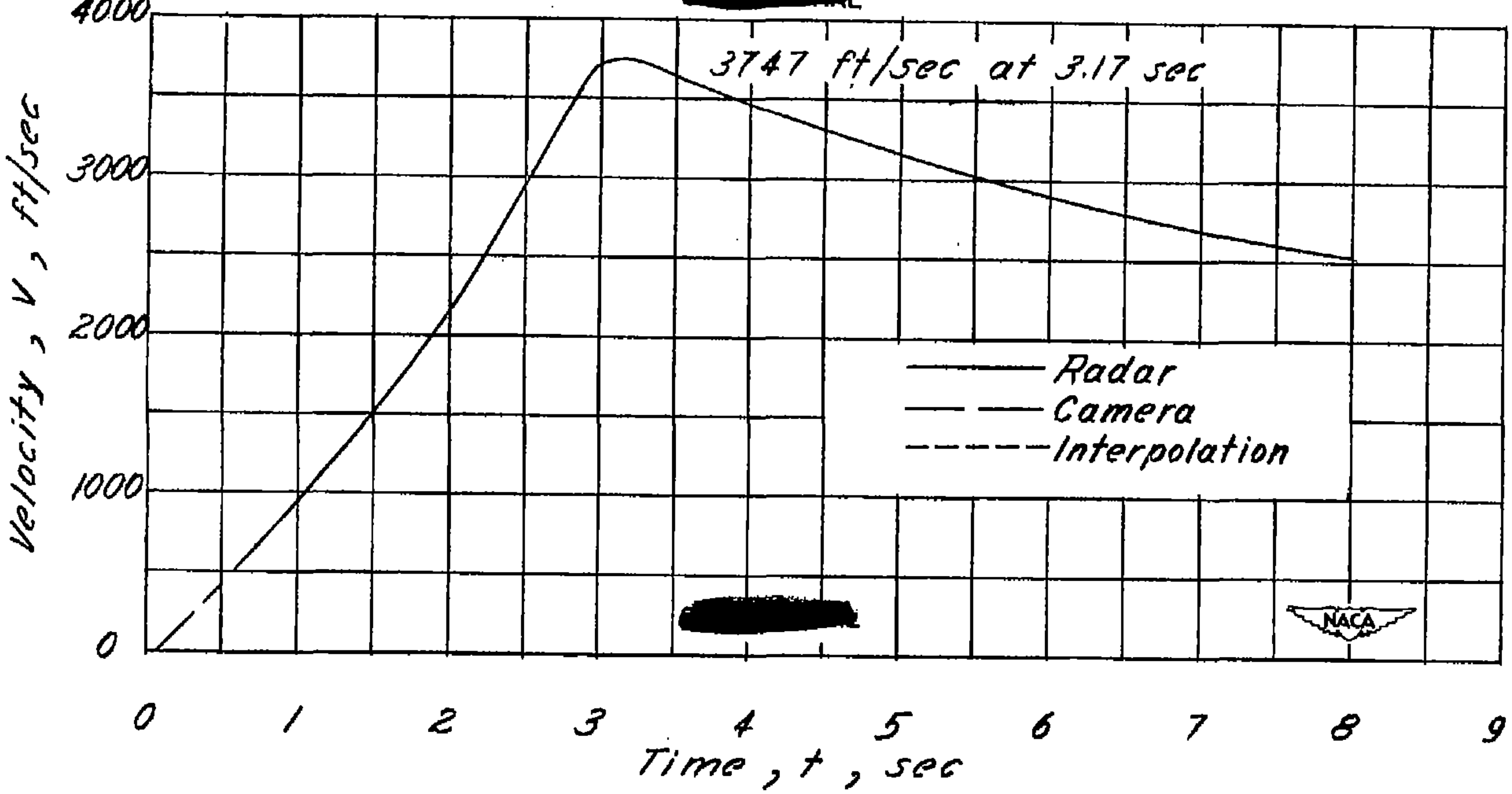

[redacted]

(c) Round 4.
Figure 2.-Continued.

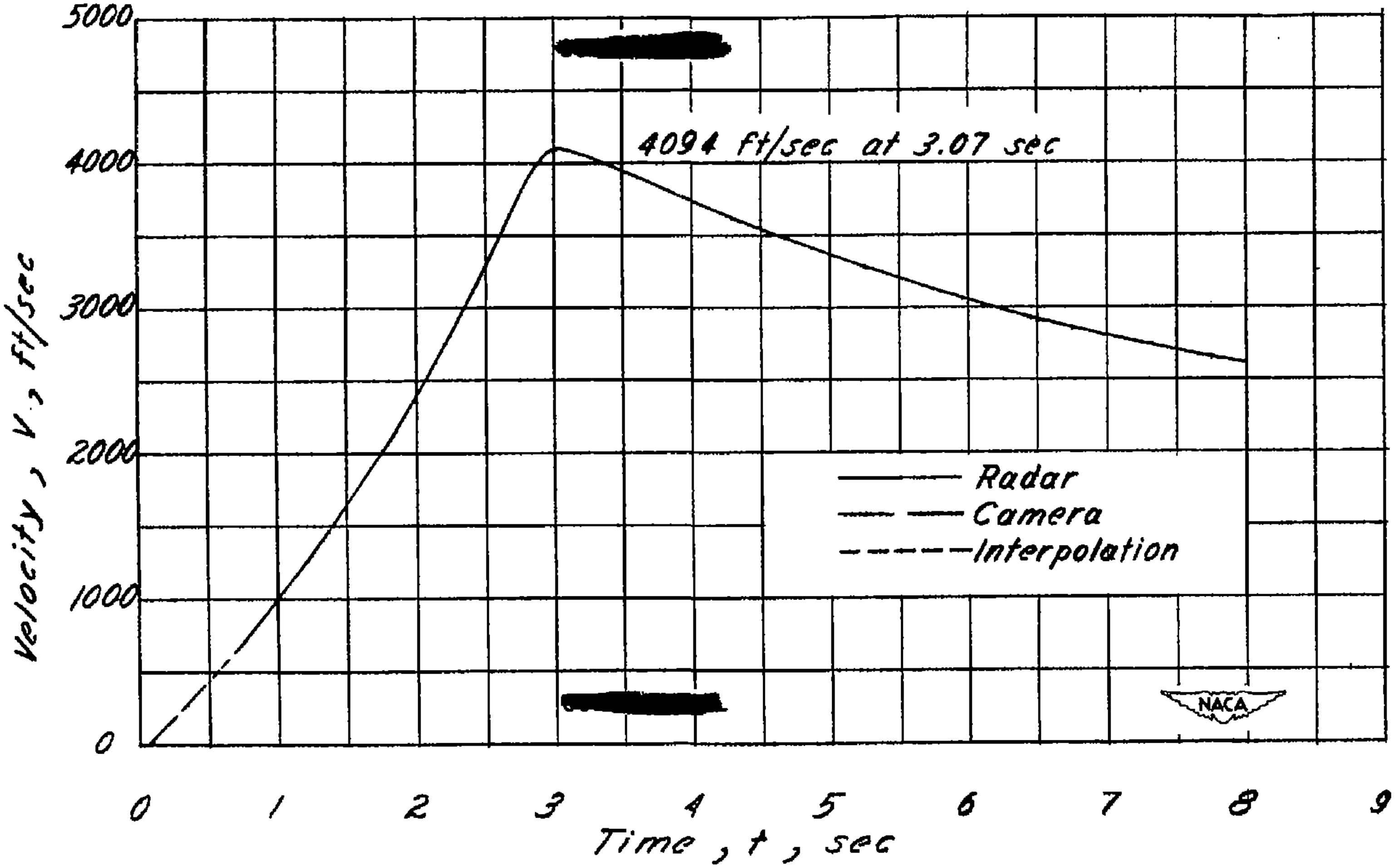

(d) Round 5.

Figure 2.- Continued.

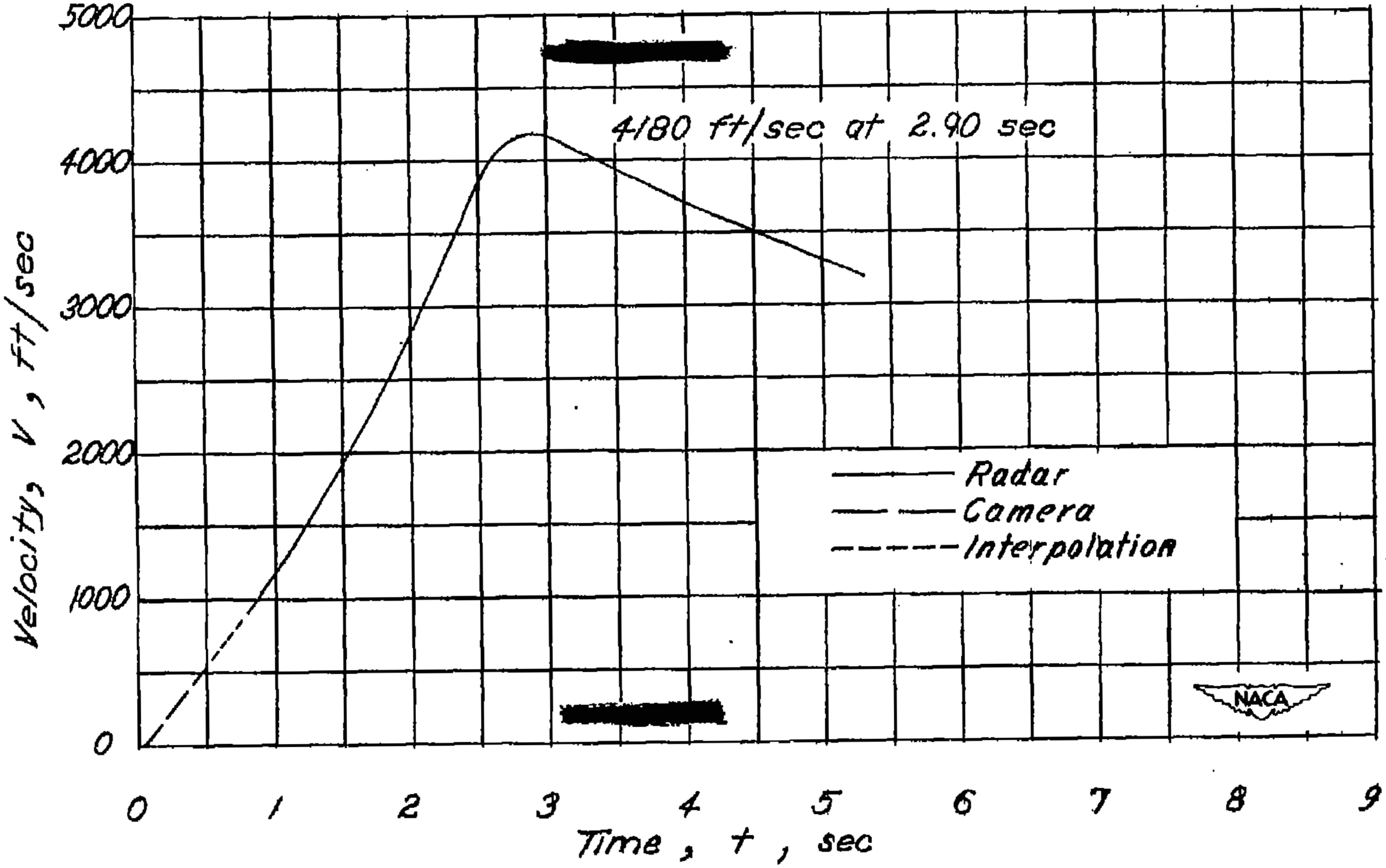

(e) Round 6.
Figure 2.– Continued.

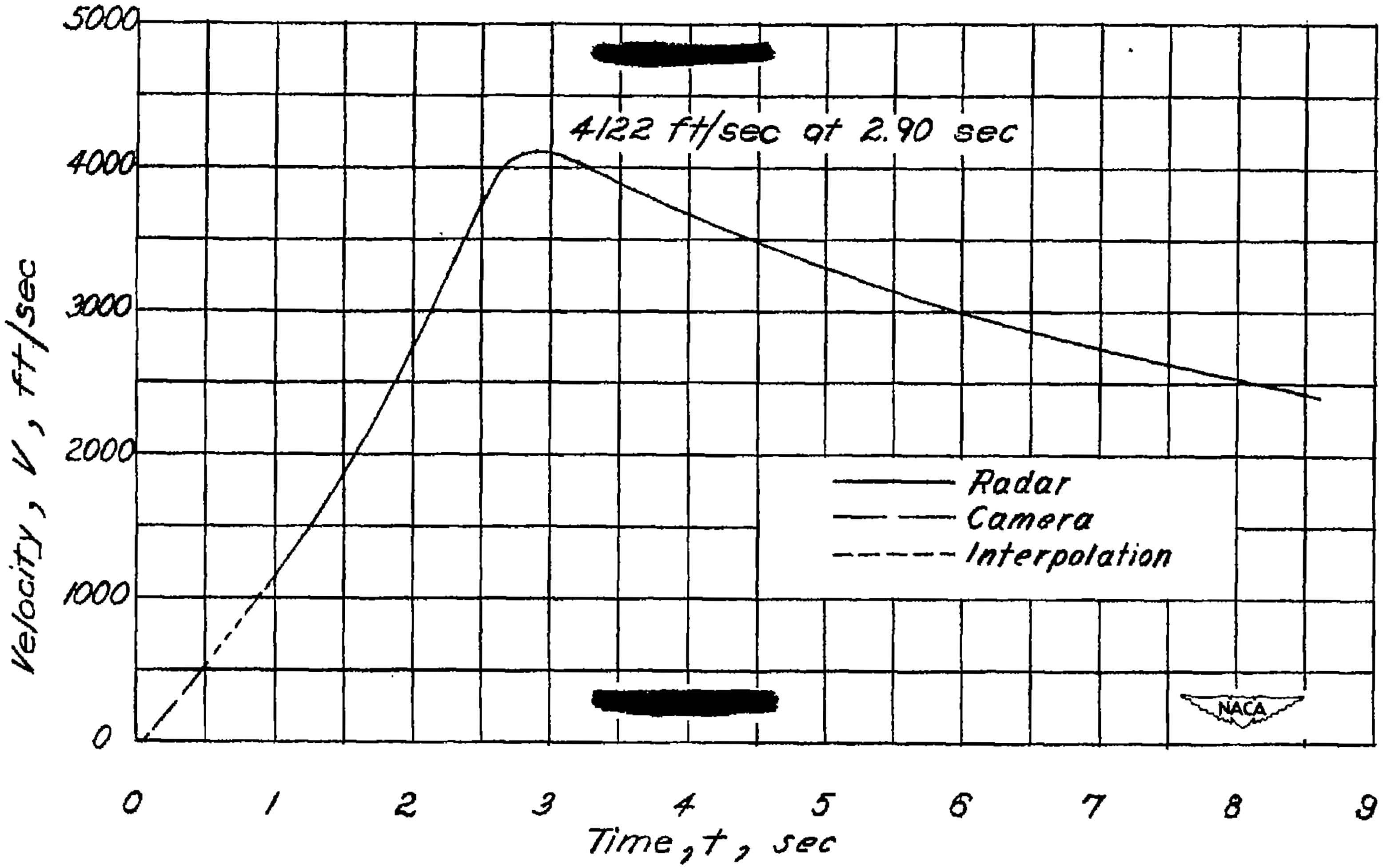

(f) Round 7.
Figure 2. - Continued.

[redacted]

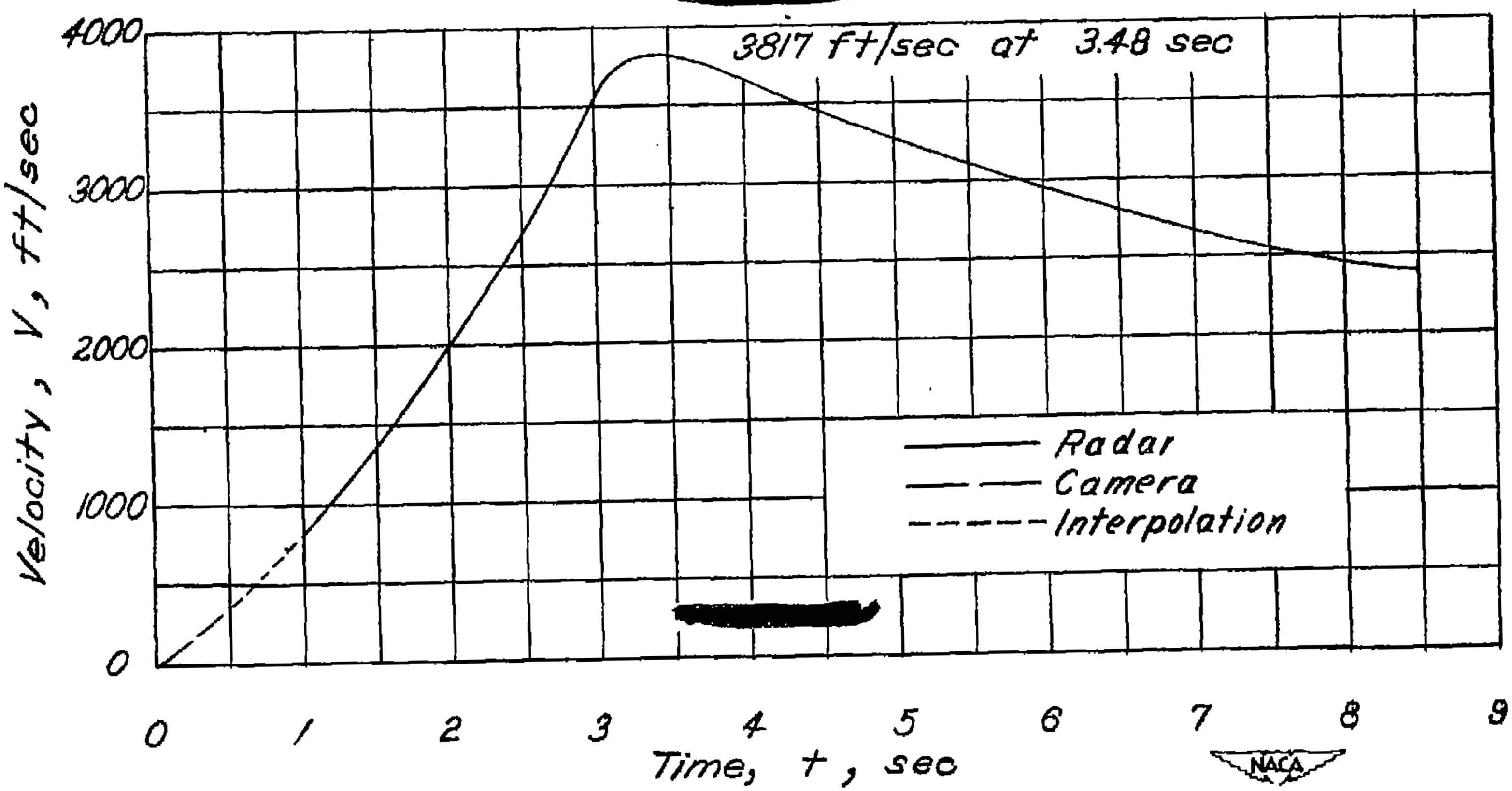

[redacted]

(g) Round 8.
Figure 2.- Continued.

[redacted]

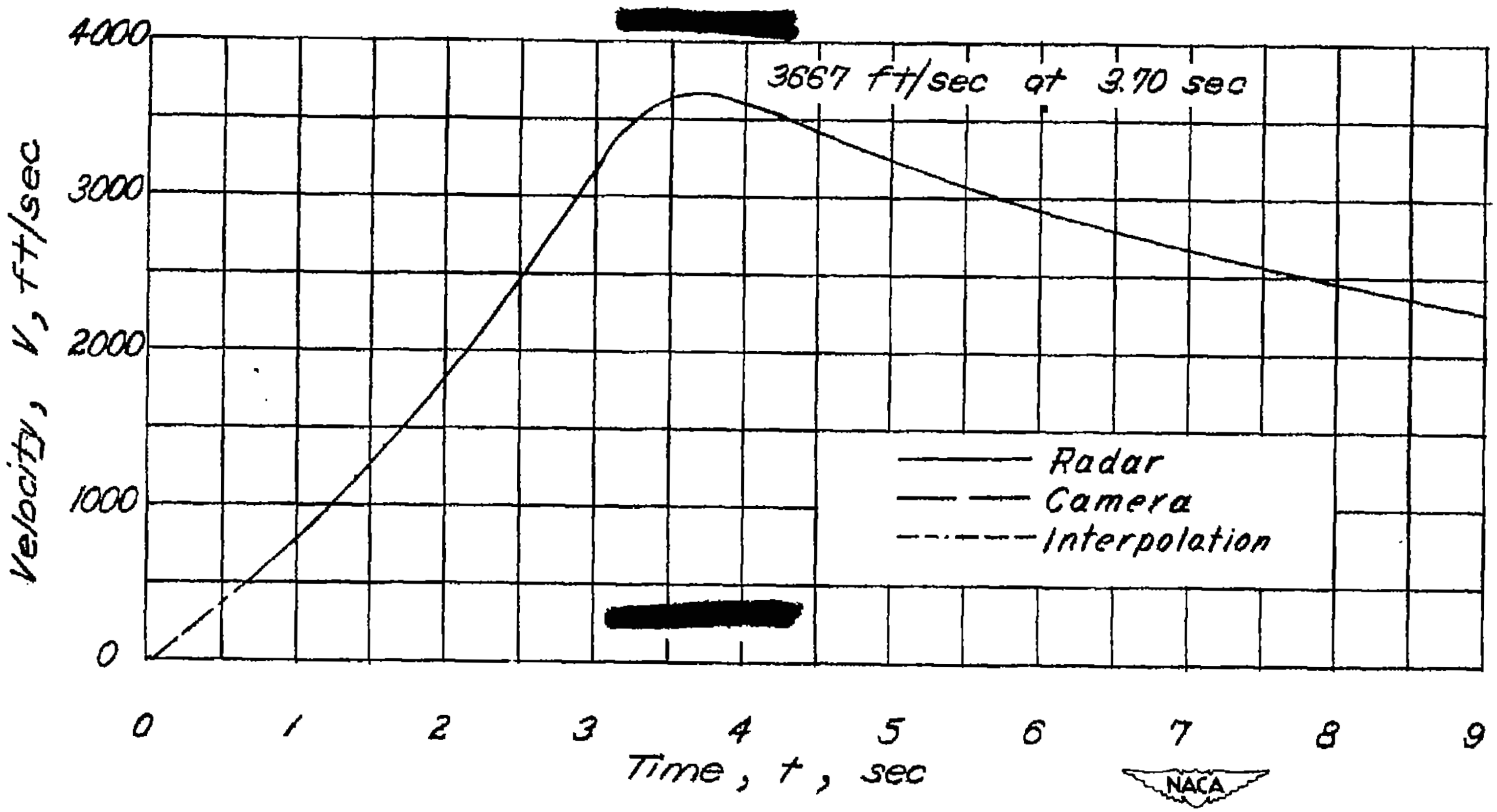

[redacted]

(h) Round 9.
Figure 2. – Continued.

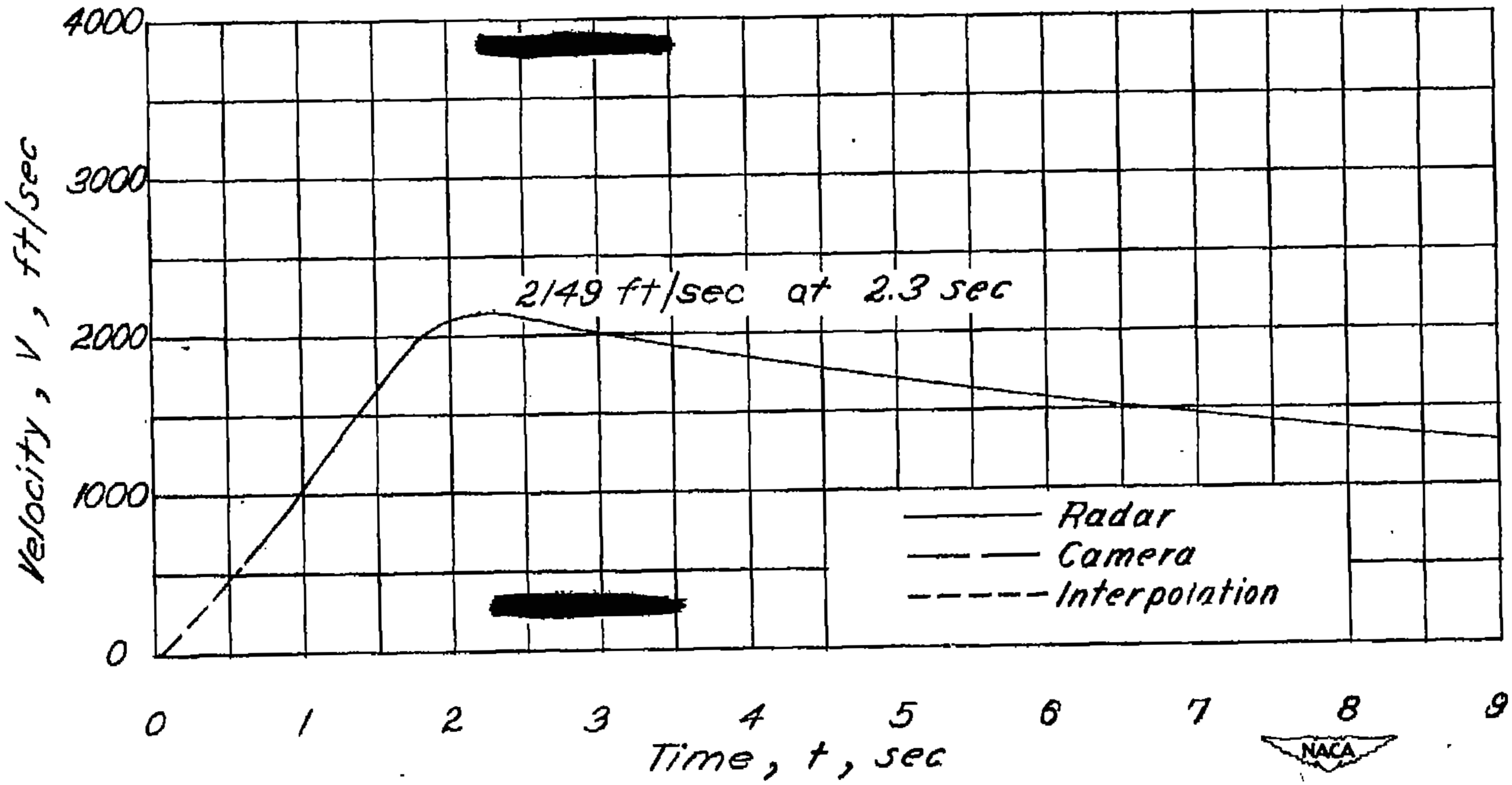

(i) Round 10.

Figure 2.—Concluded.

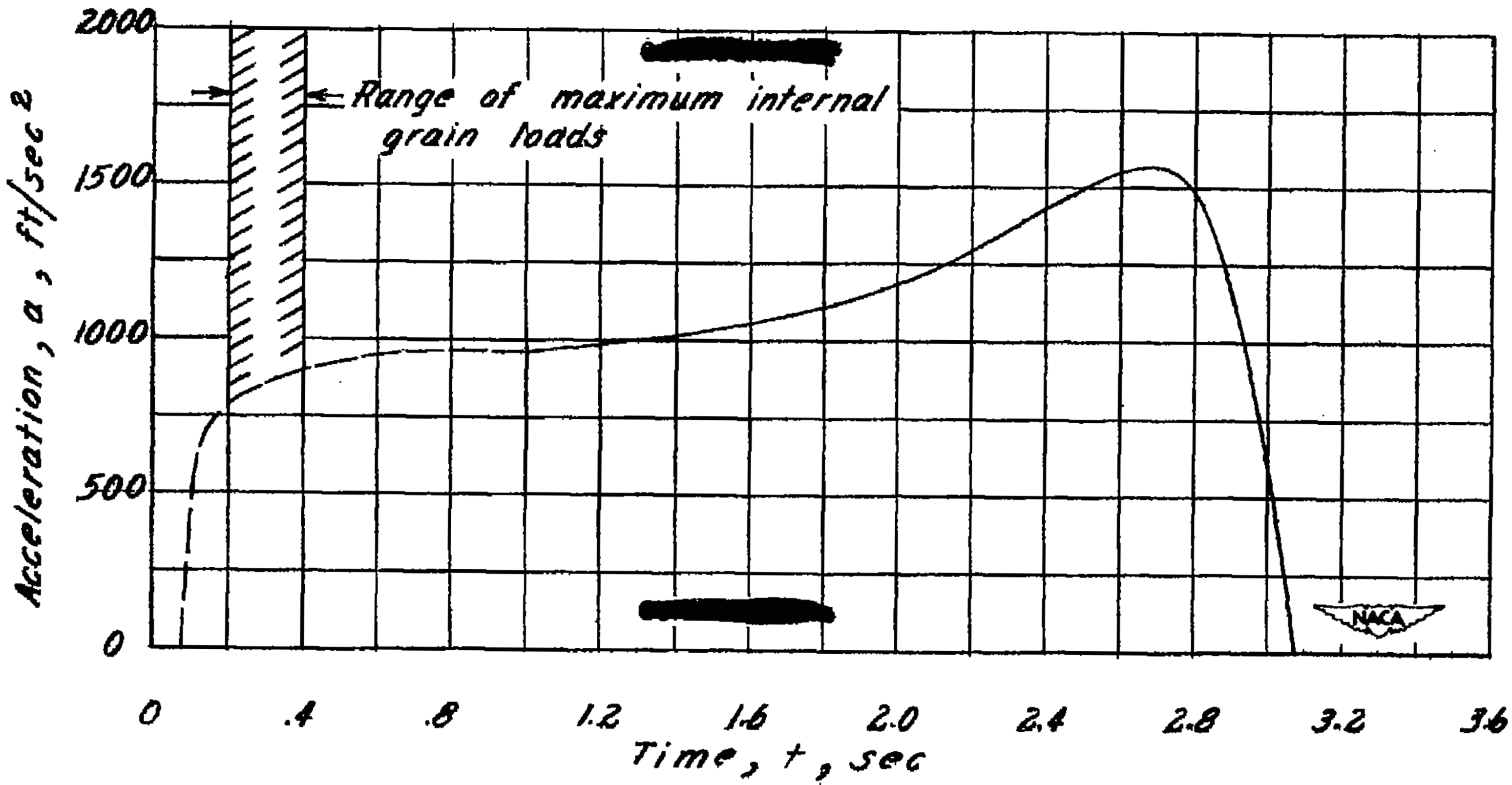

(a) Round 2.

Figure 3.- Acceleration-time curves, 6.25-inch Deacon rocket motor.

[redacted]

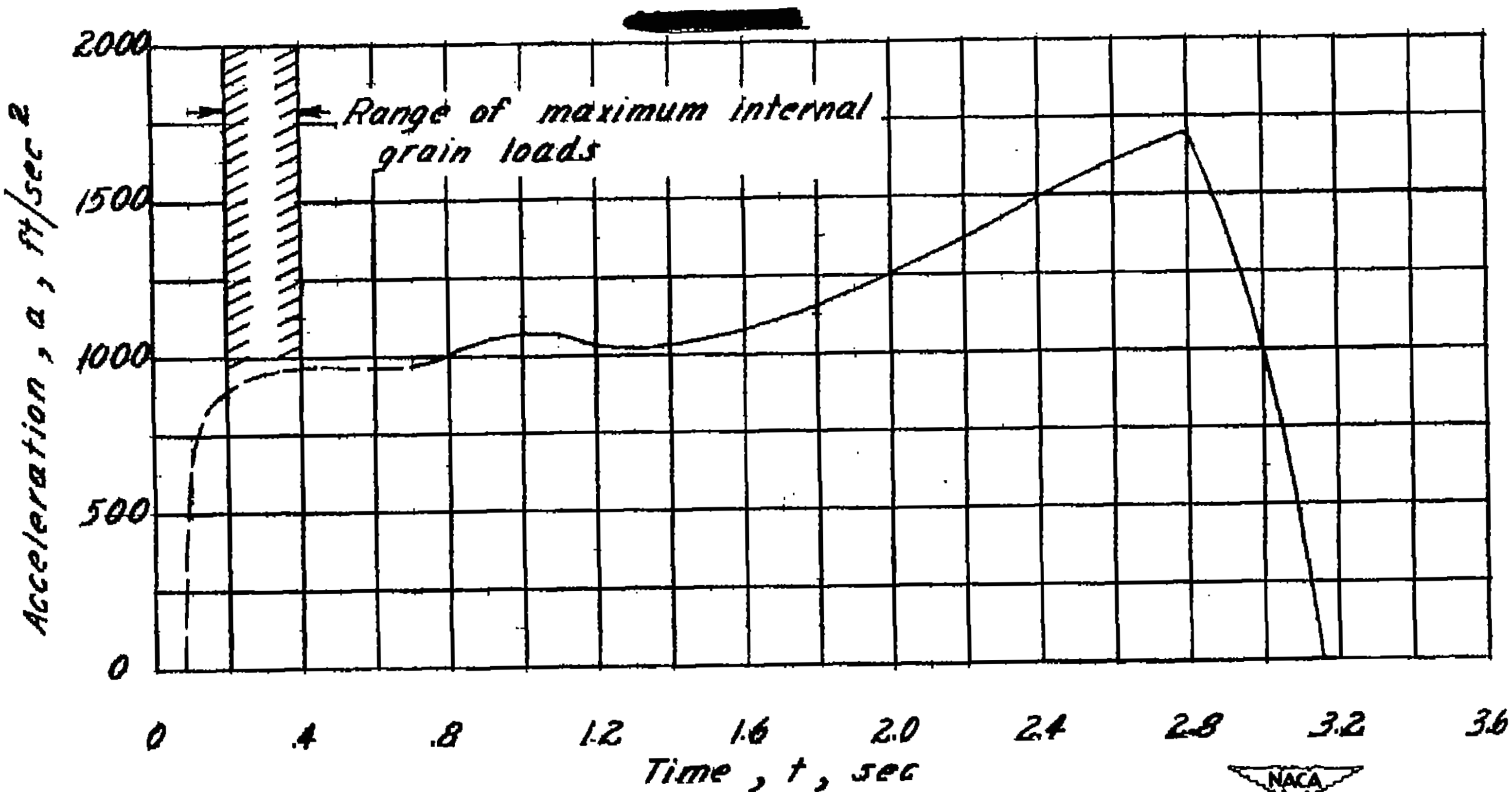

[redacted]

(b) Round 3.

Figure 3.- Continued.

[redacted]

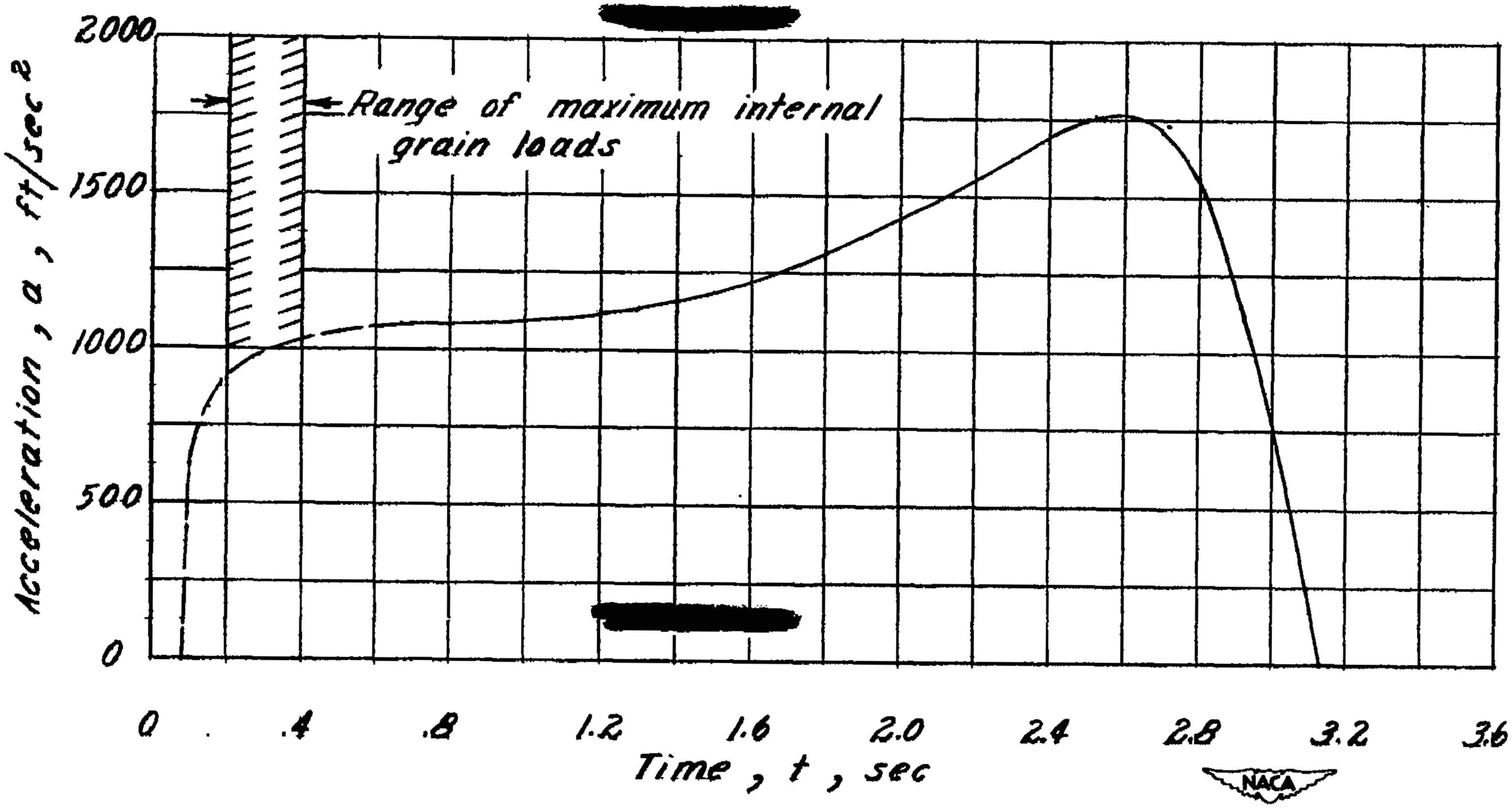

[redacted]

(c) Round 4.
Figure 3.- Continued.

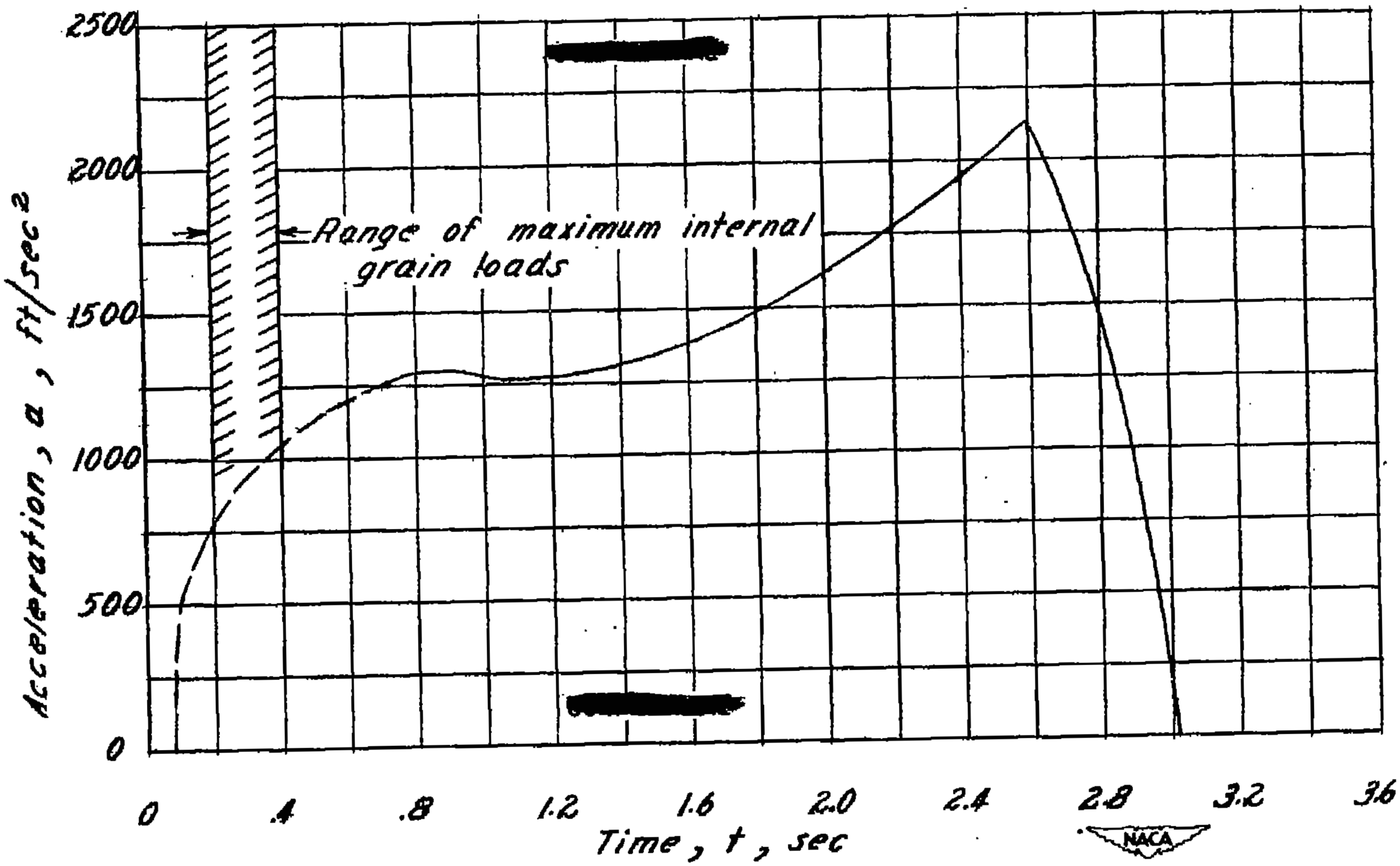

(d) Round 5.
Figure 3.- Continued.

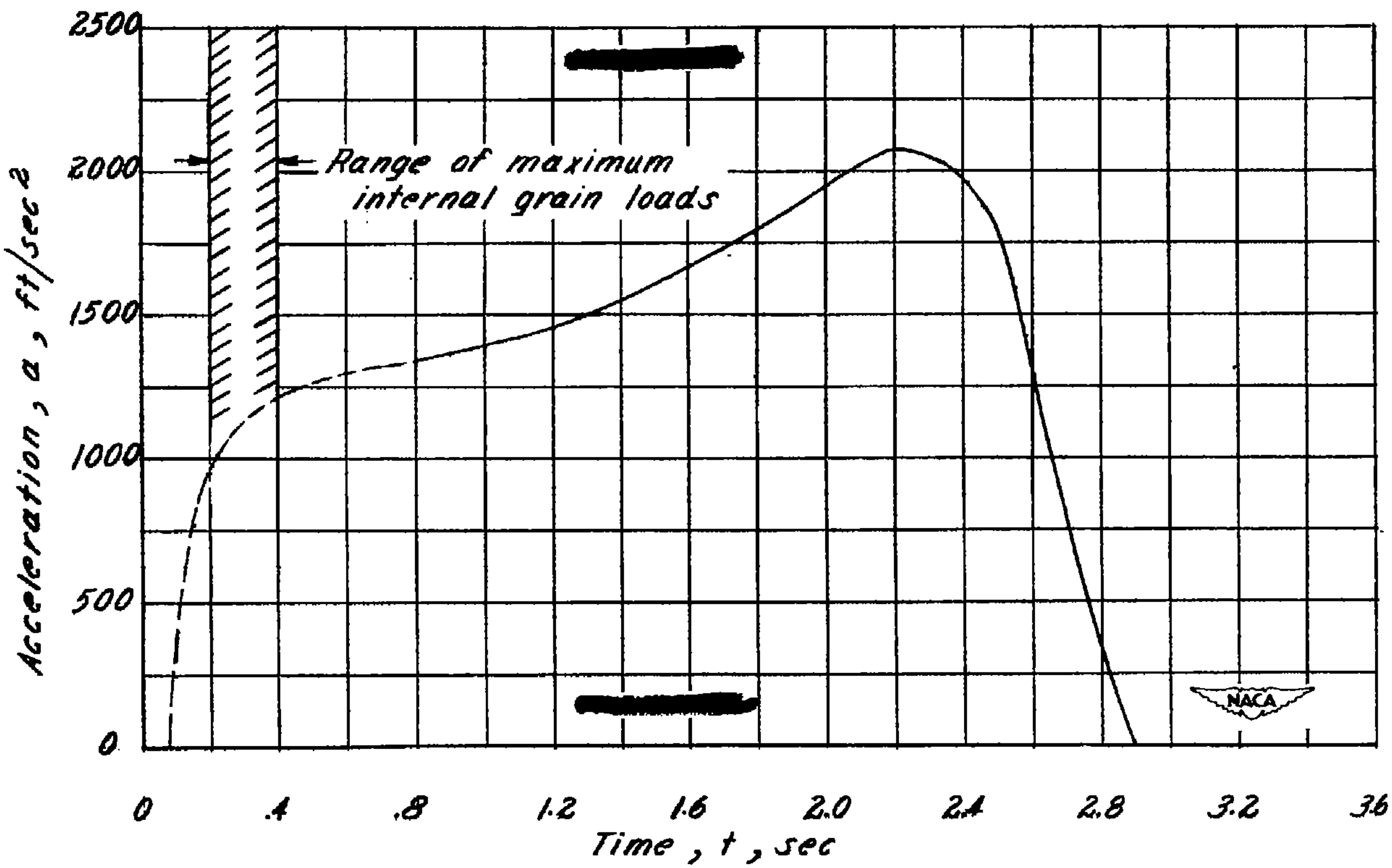

(e) Round 6.

Figure 3.- Continued.

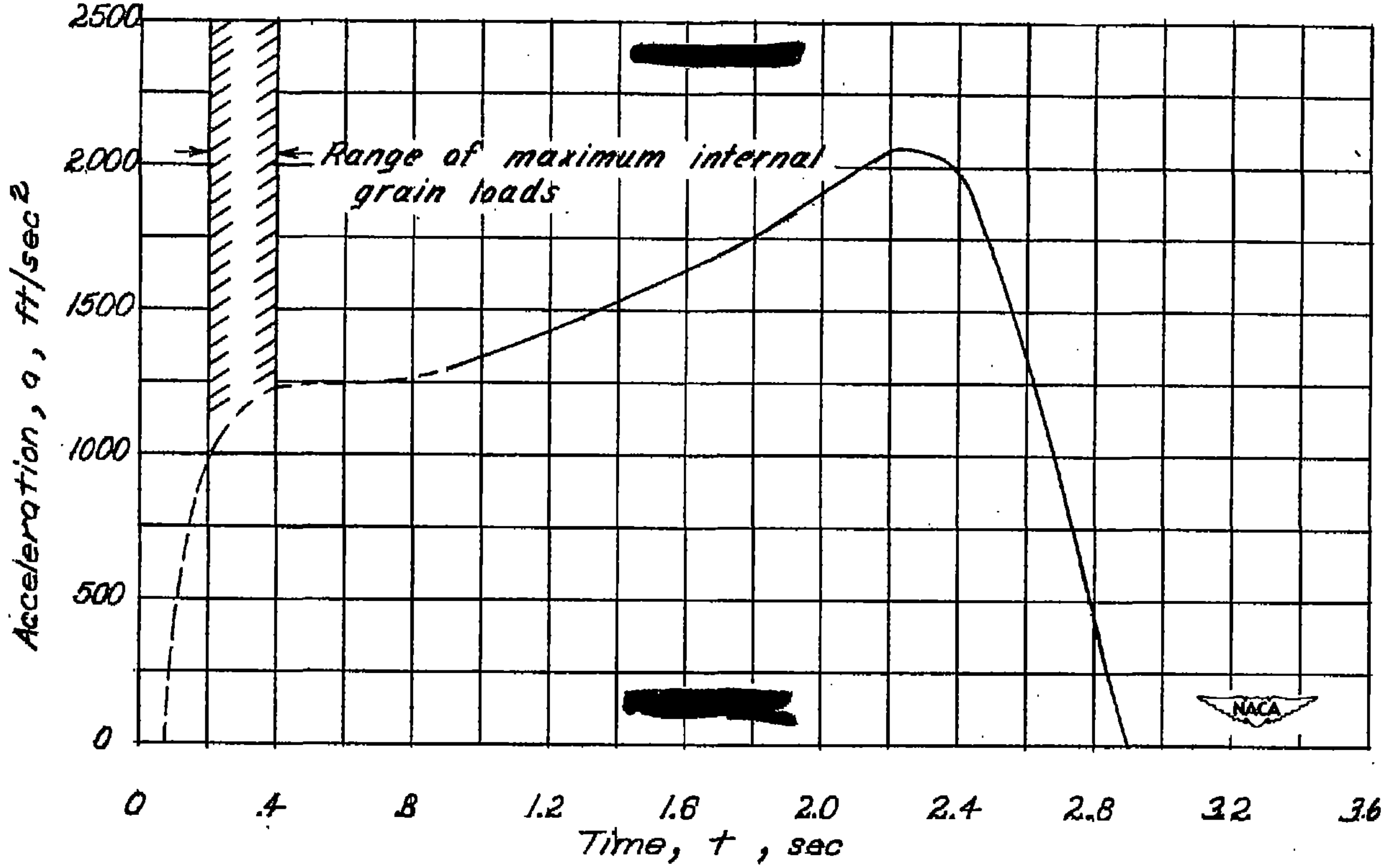

(f) Round 7.
Figure 3. - Continued.

[redacted]

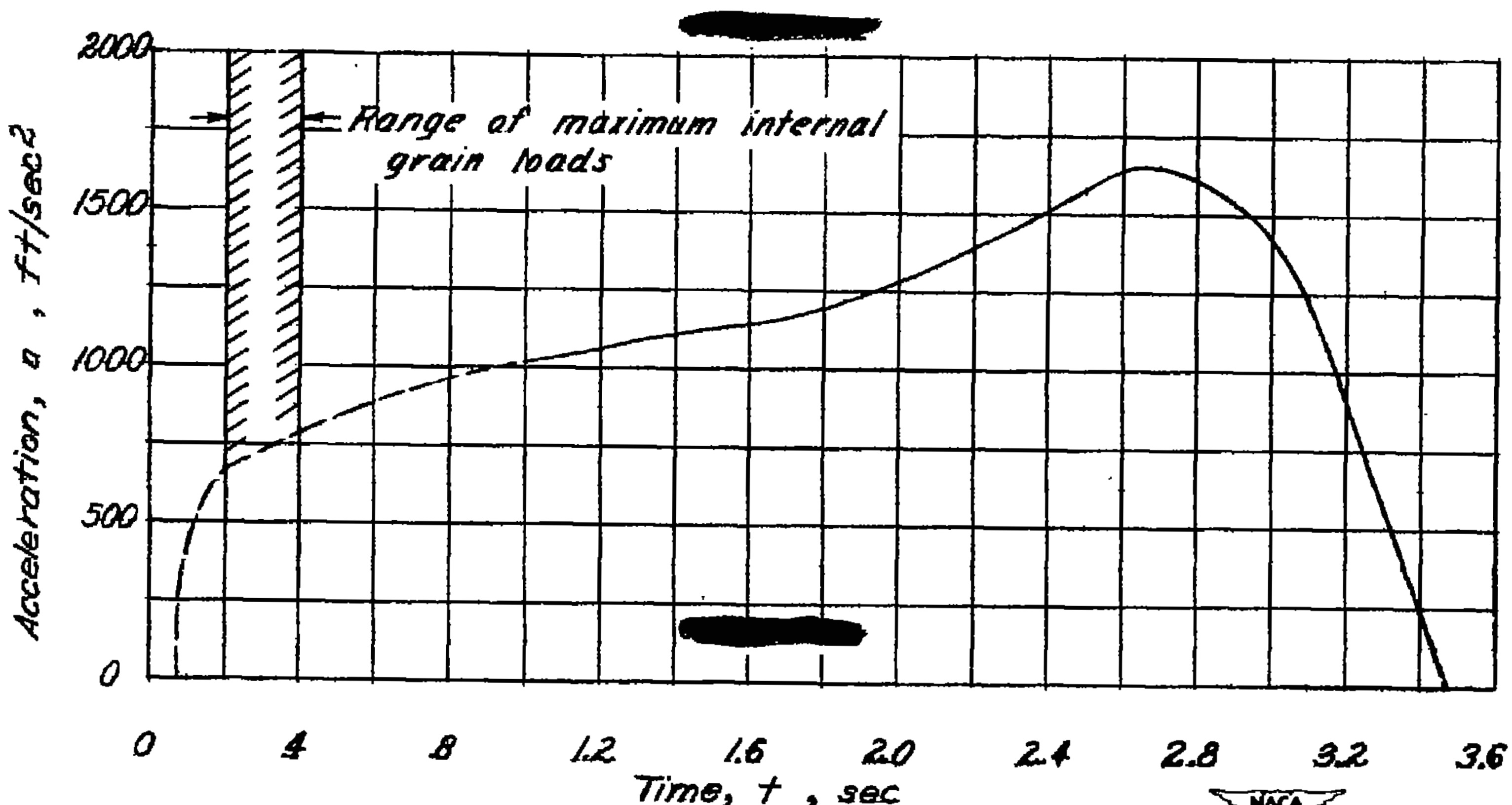

[redacted]

(g) Round 8.
Figure 3. - Continued.

[redacted]

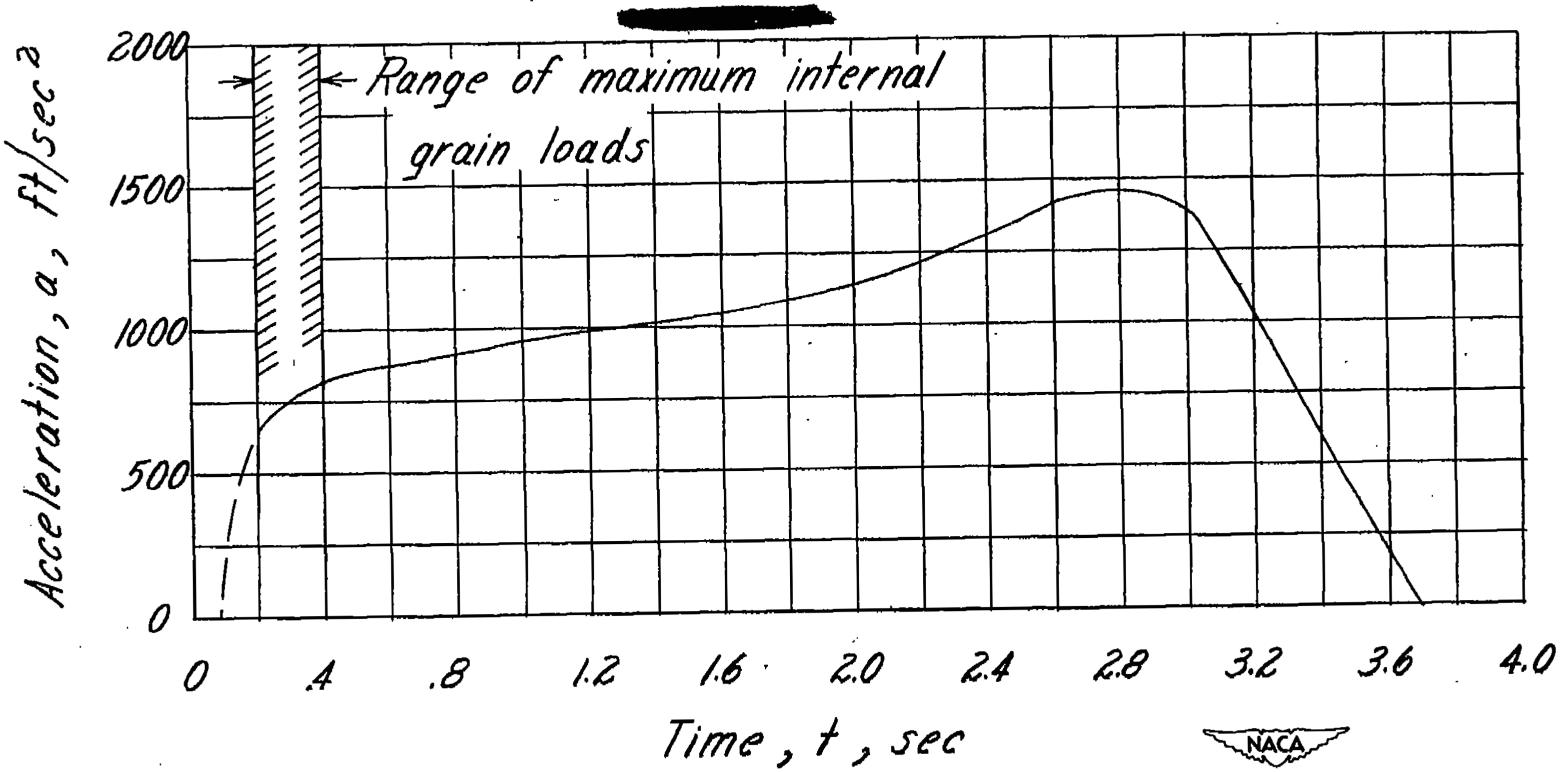

[redacted]

(h) Round 9.

Figure 3.-Continued.

[redacted]

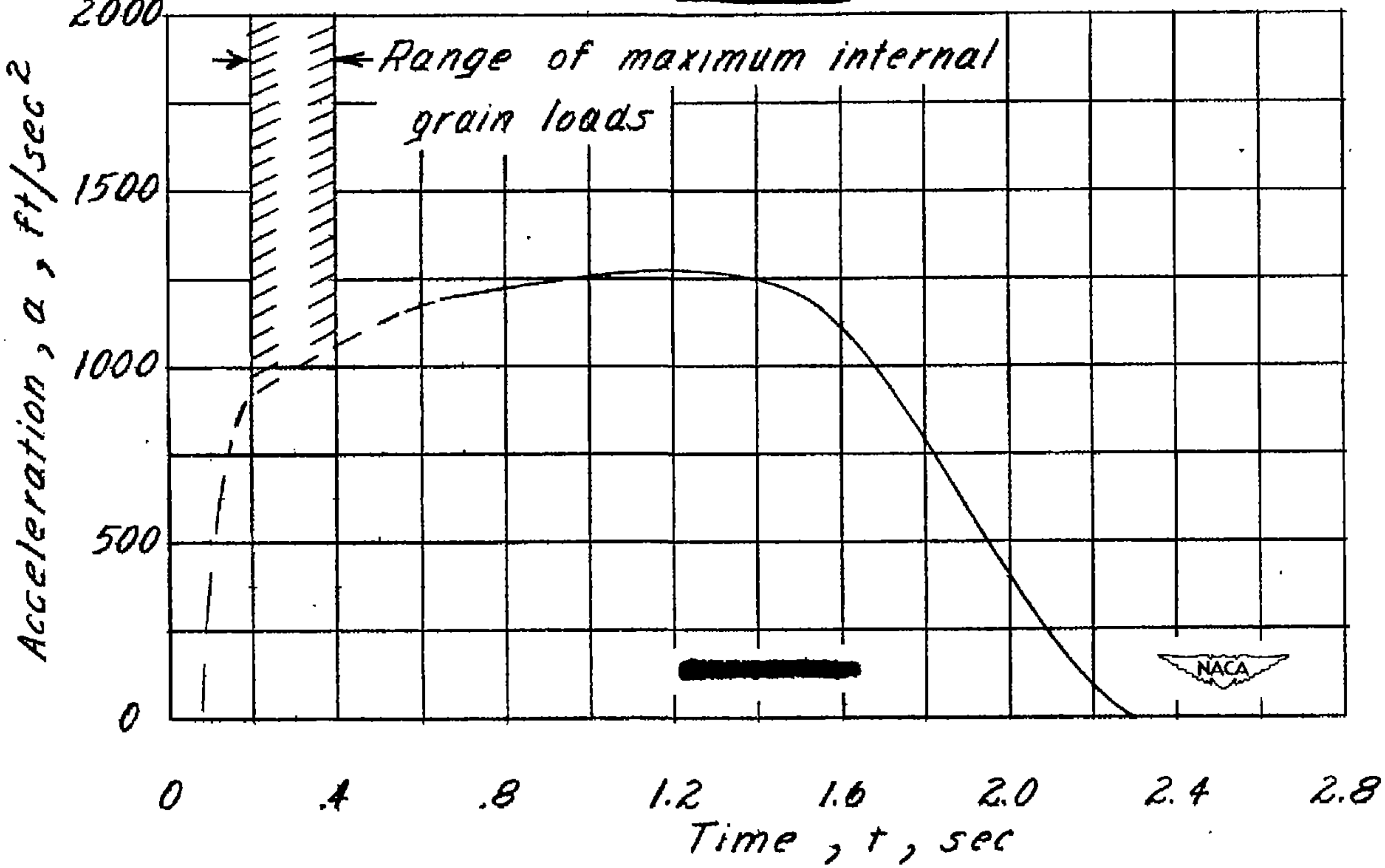

[redacted]

(i) Round 10.

Figure 3.- Concluded.

[redacted]

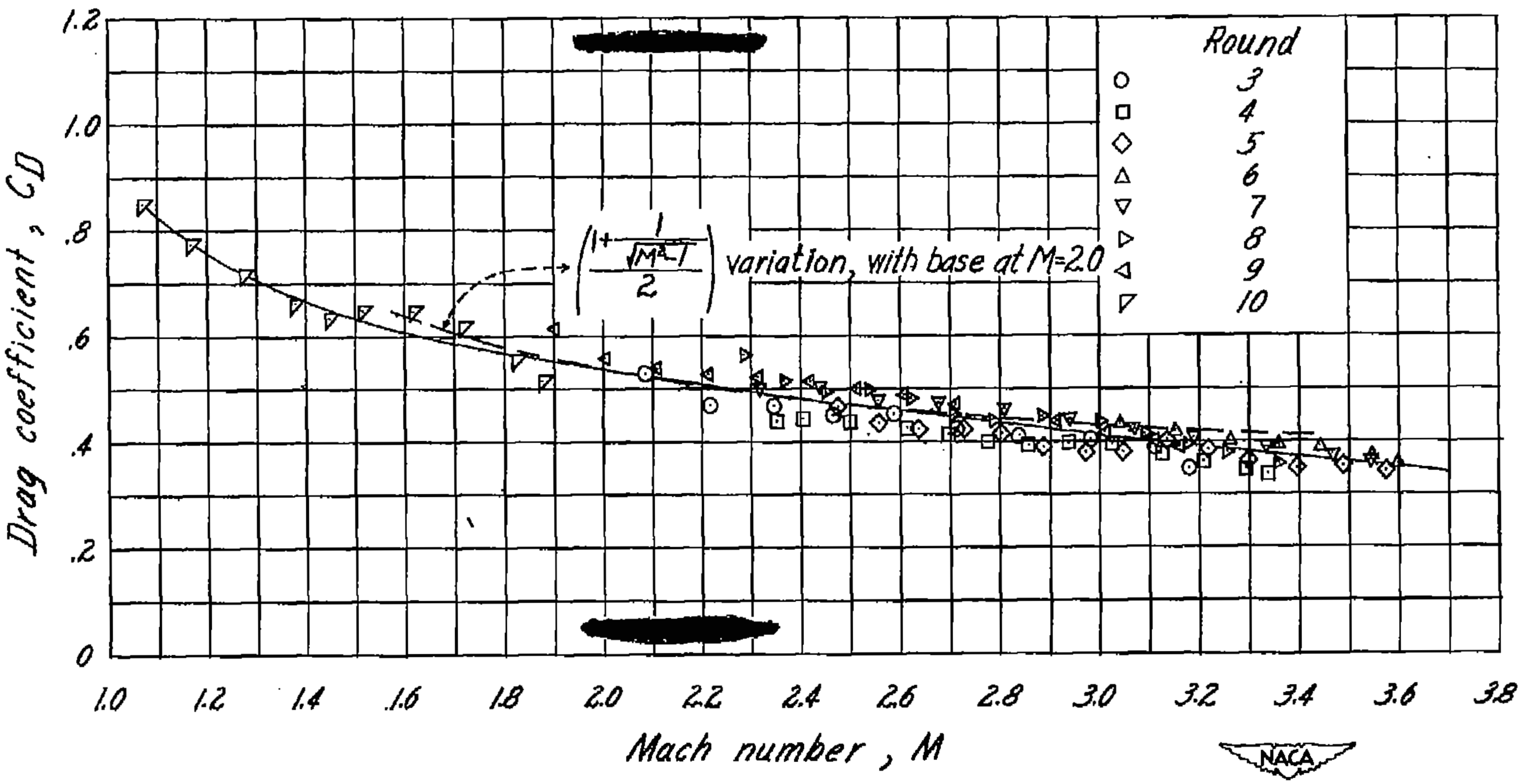

[redacted]

Figure 4.- Drag coefficient for the 6.25-inch Deacon rocket motor.

[redacted]

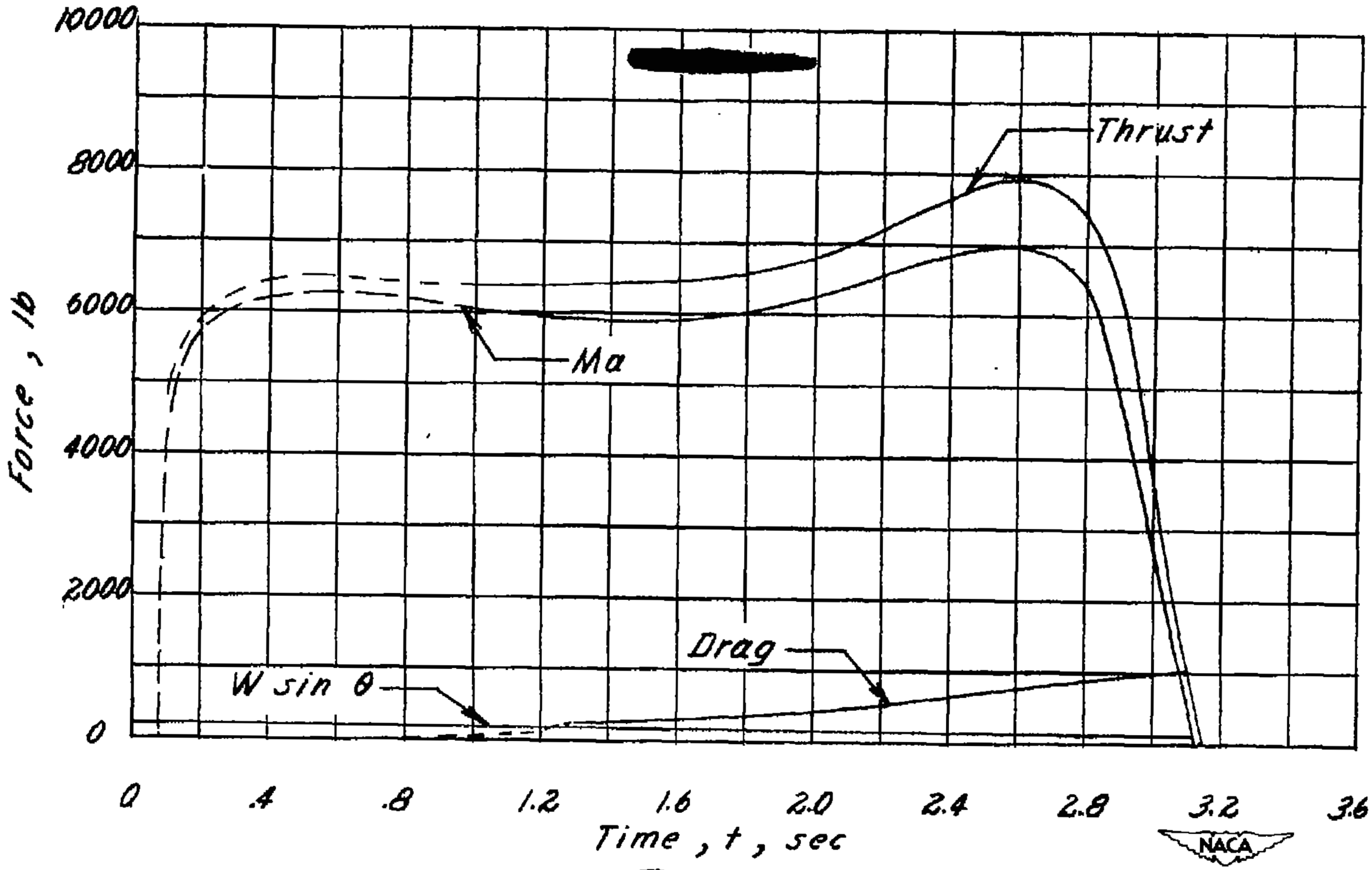

[redacted]

(a) Round 2.

Figure 5.- Force-time curves, 6.25-inch Deacon rocket motor.

[redacted]

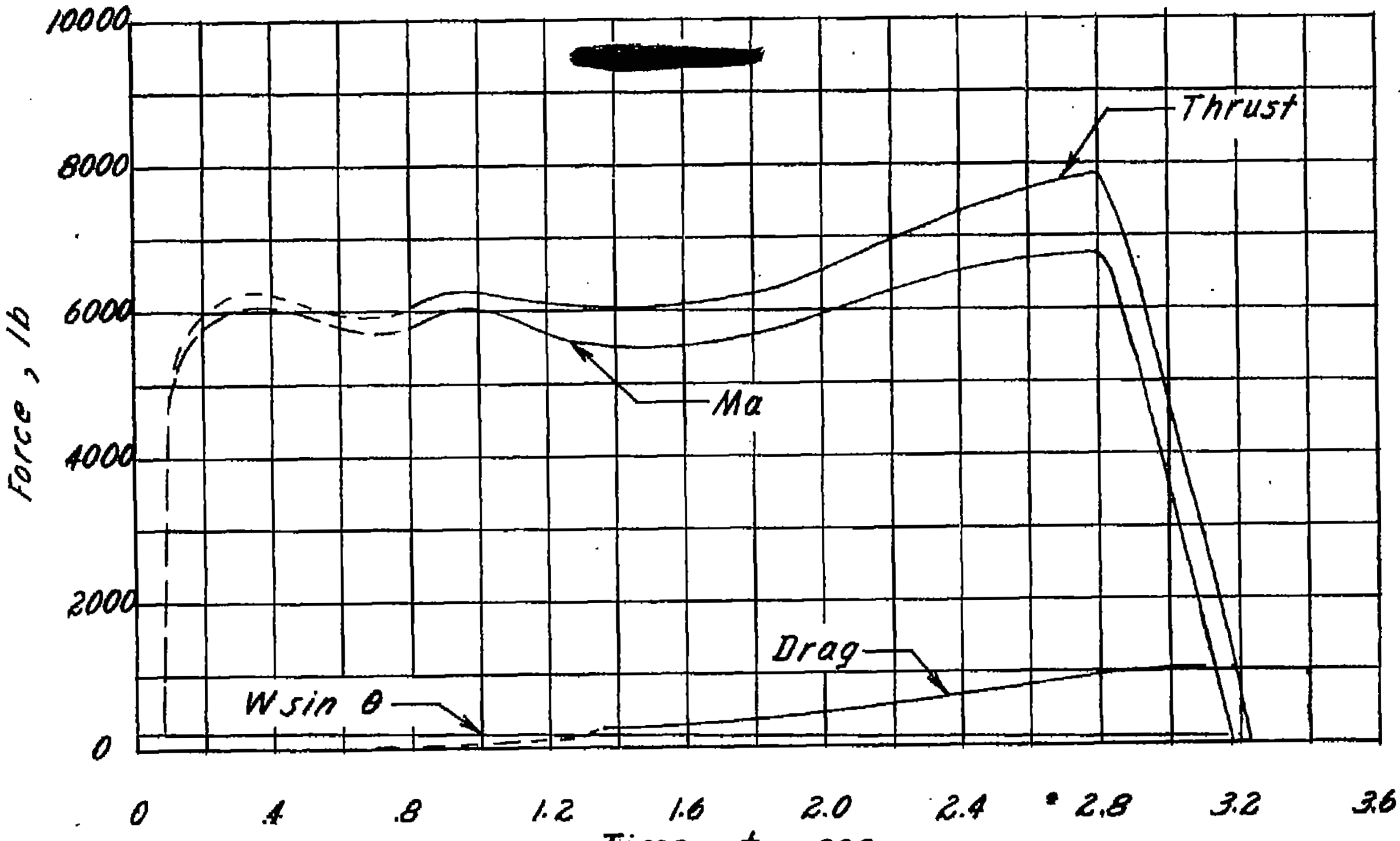

[redacted]

(b) Round 3.
Figure 5.- Continued.

[redacted]

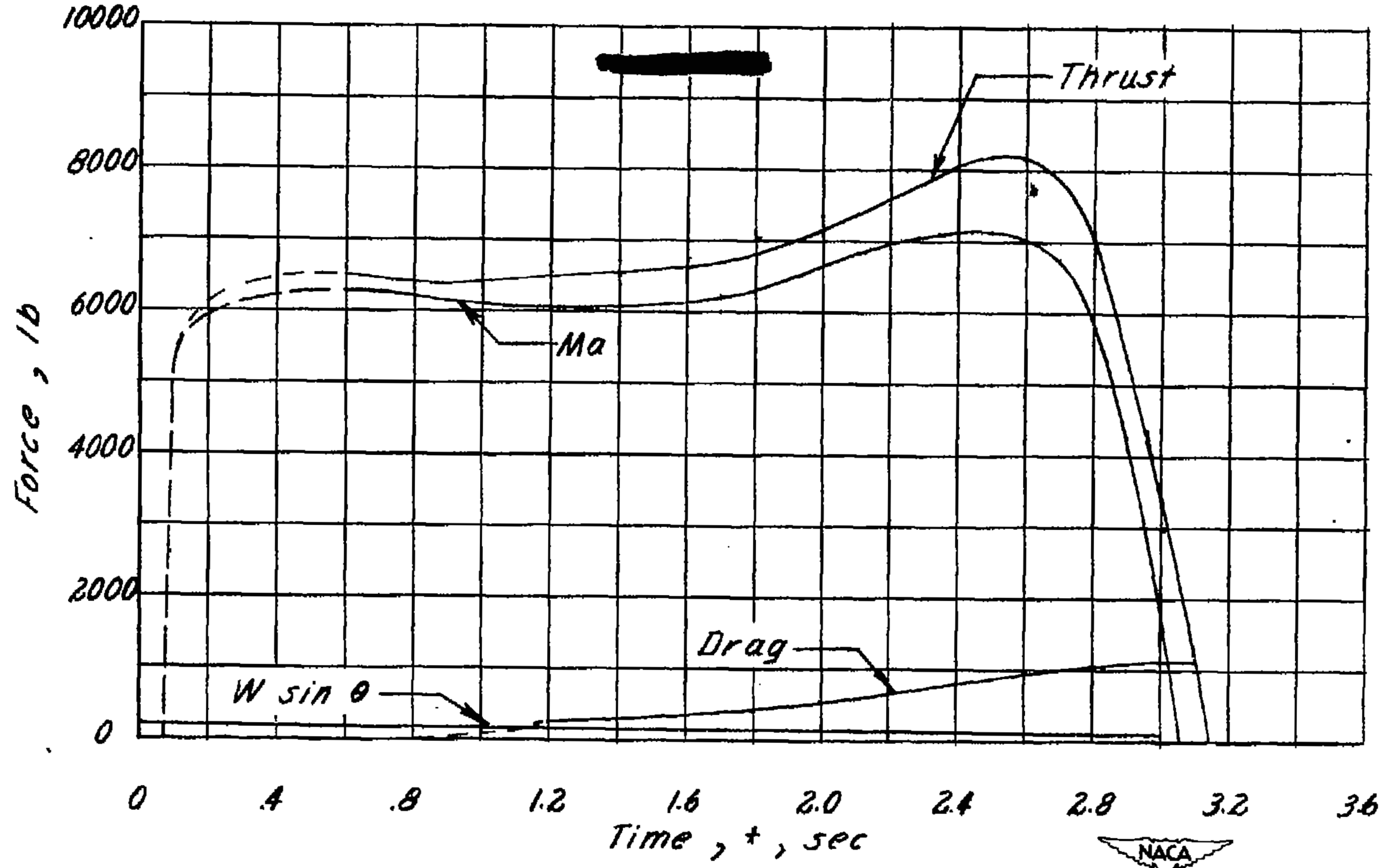

[redacted]

(c) Round 4.
Figure 5. - Continued.

[redacted]

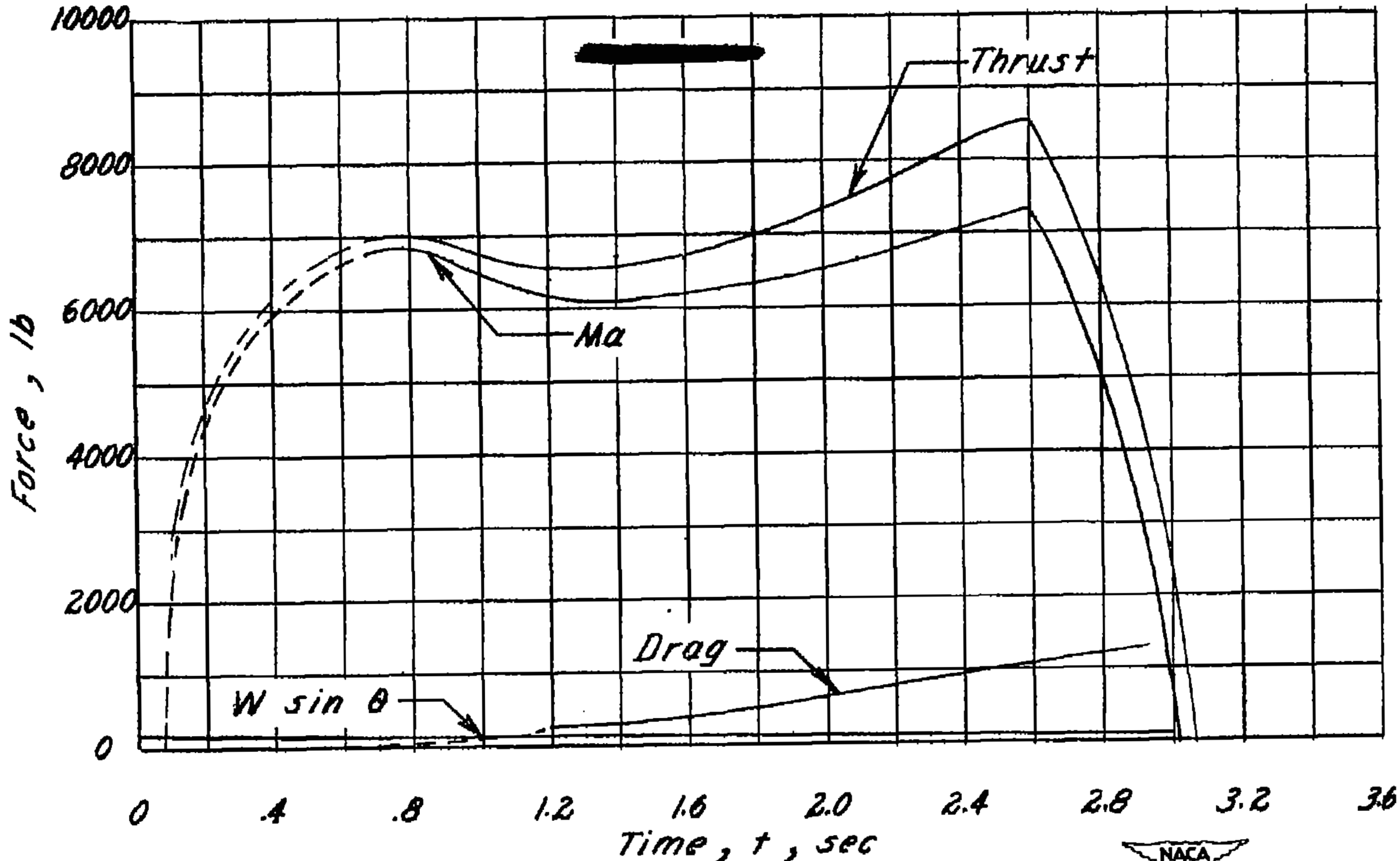

[redacted]

(d) Round 5.
Figure 5.- Continued.

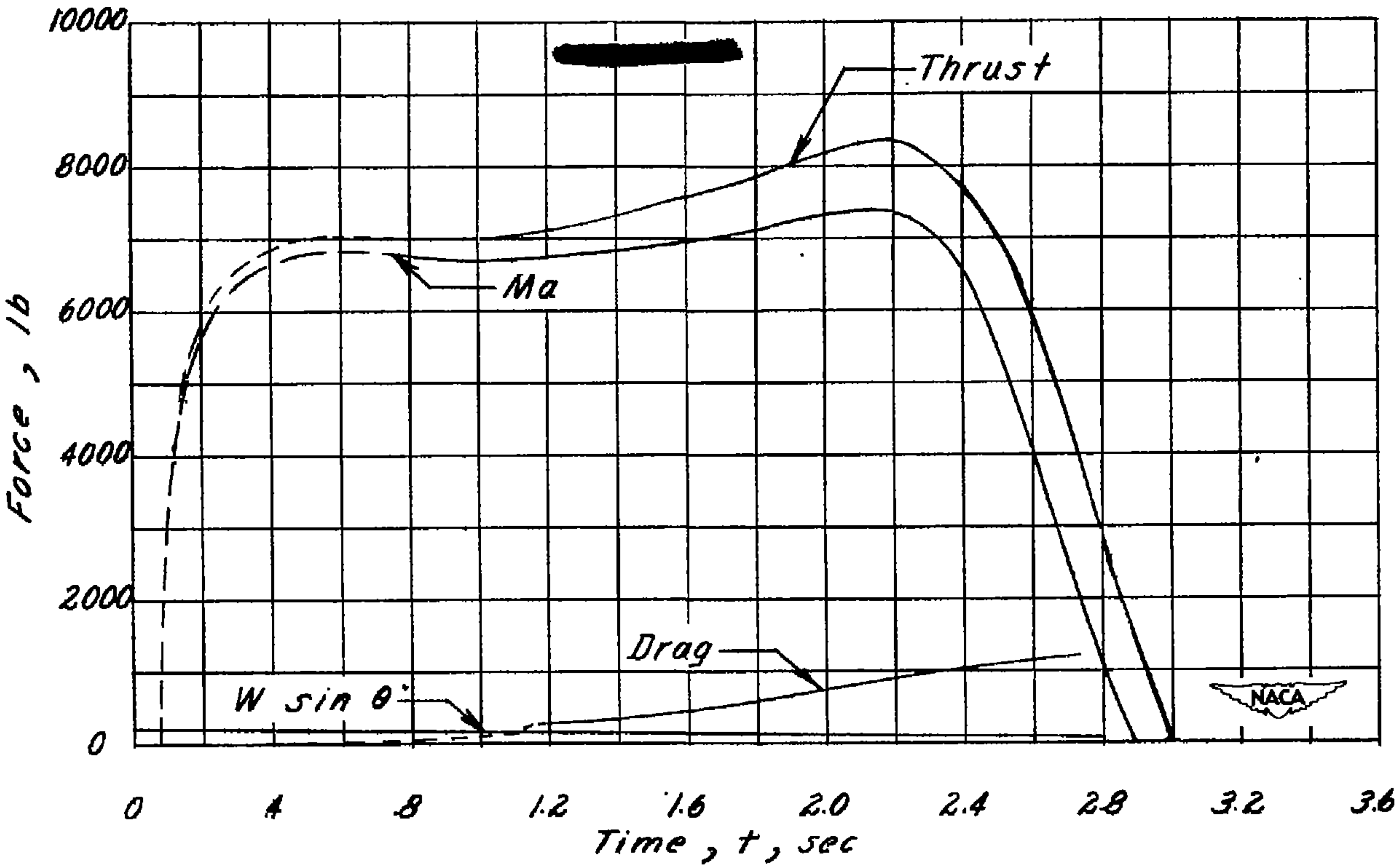

[redacted]

(e) Round 6.

Figure 5.- Continued.

[redacted]

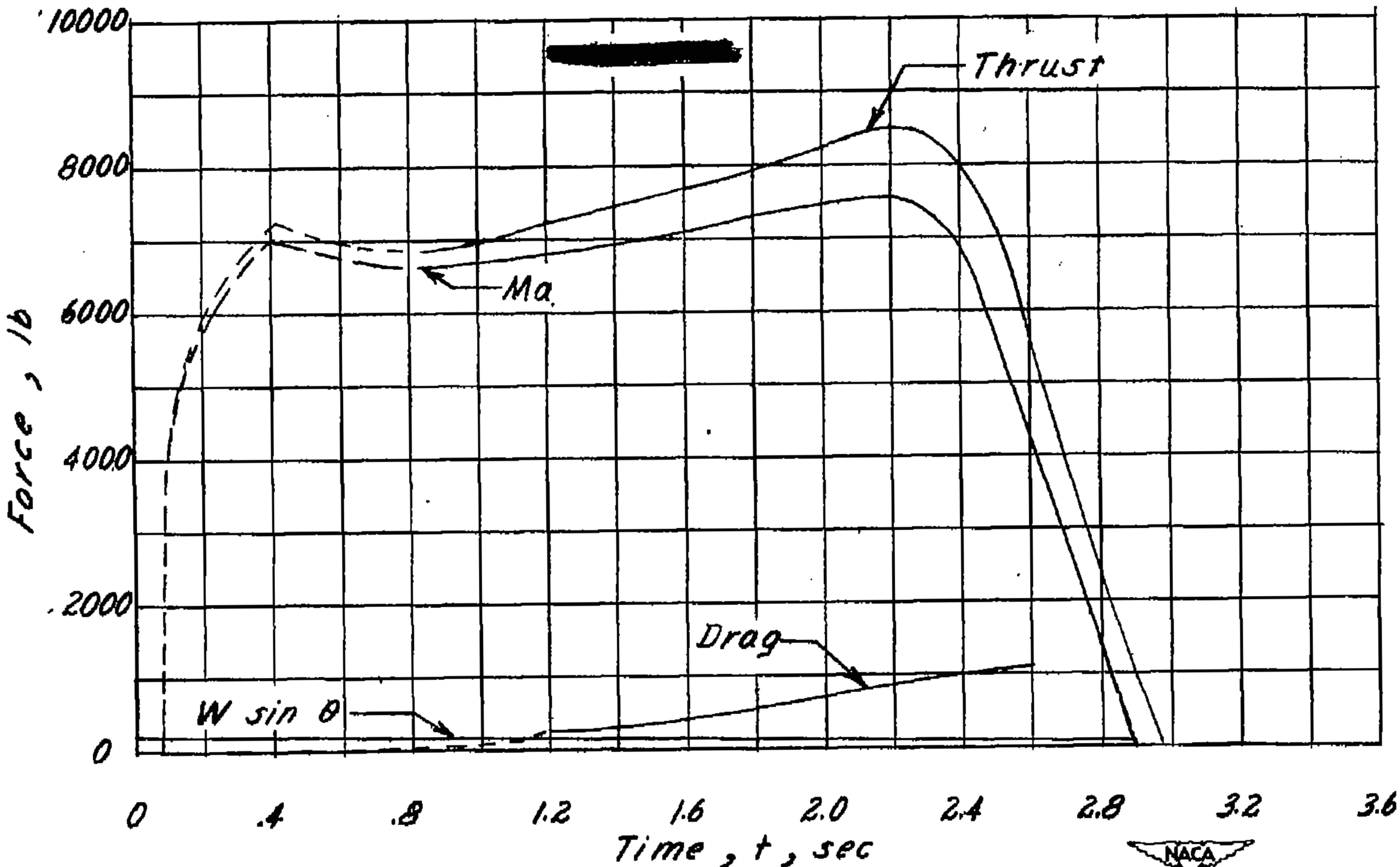

[redacted]

(f) Round 7.
Figure 5.- Continued.

[redacted]

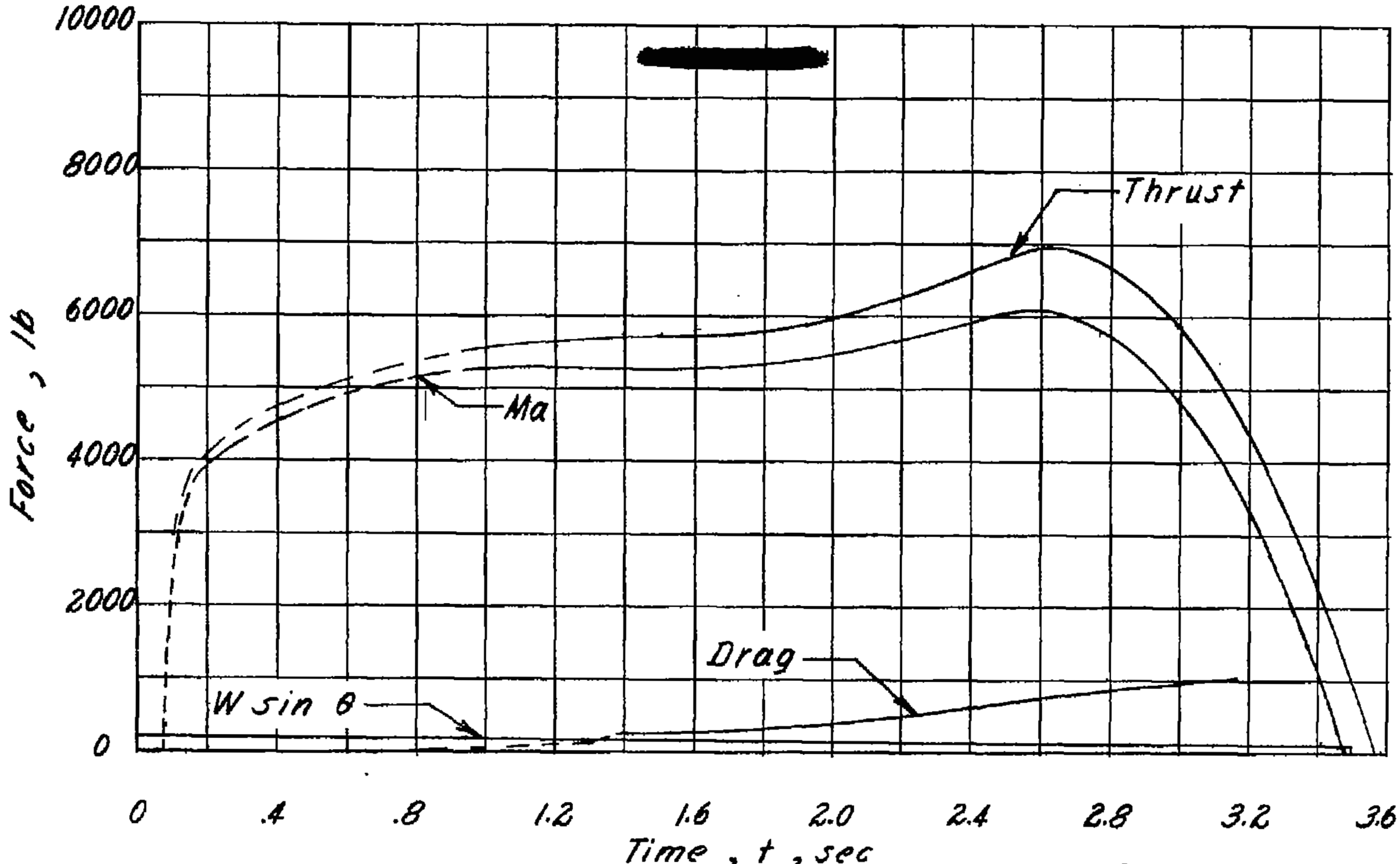

[redacted]

(g) Round 8.

Figure 5.- Continued.

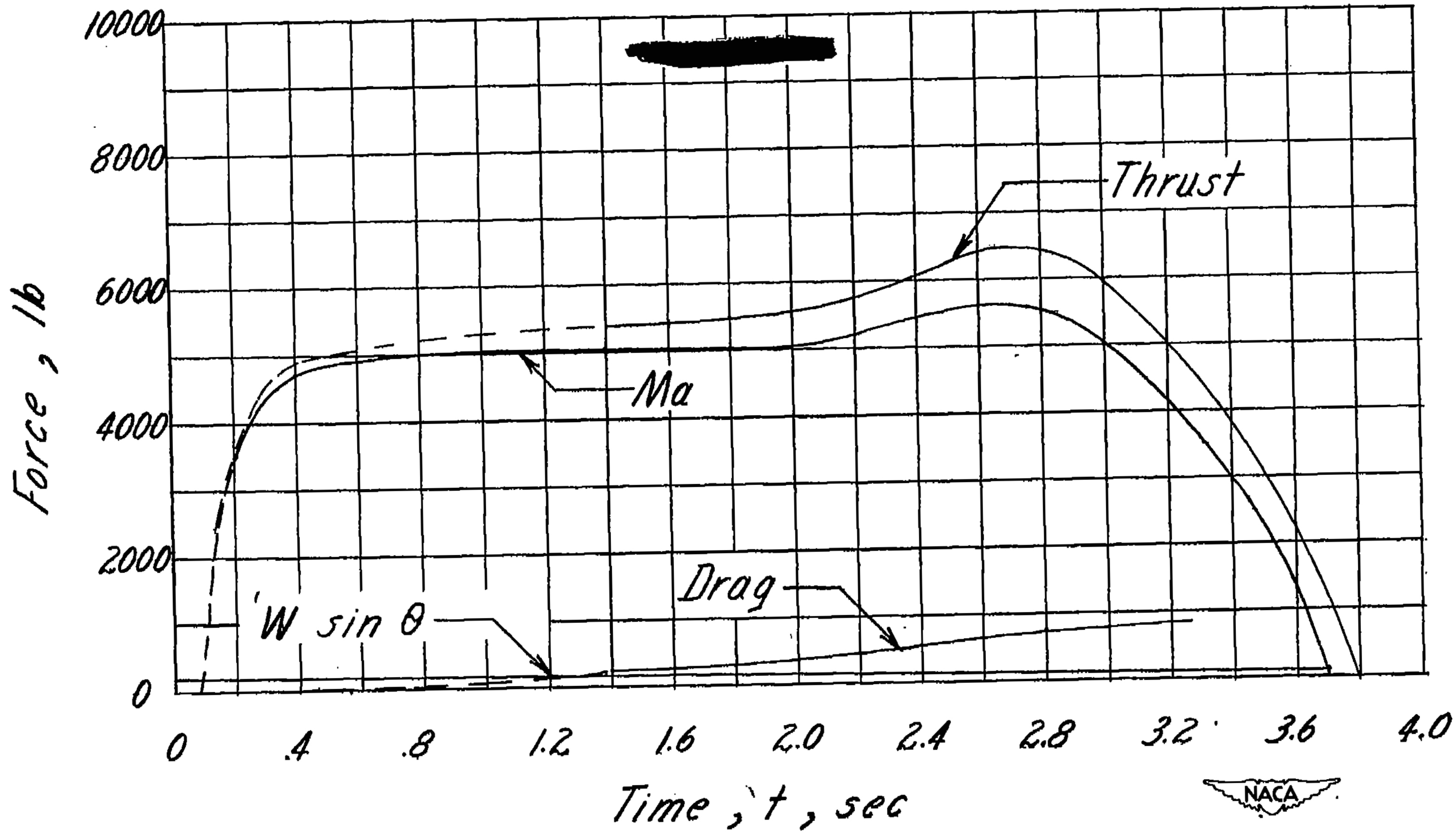

[redacted]

(h) Round 9.

Figure 5.- Continued.

[redacted]

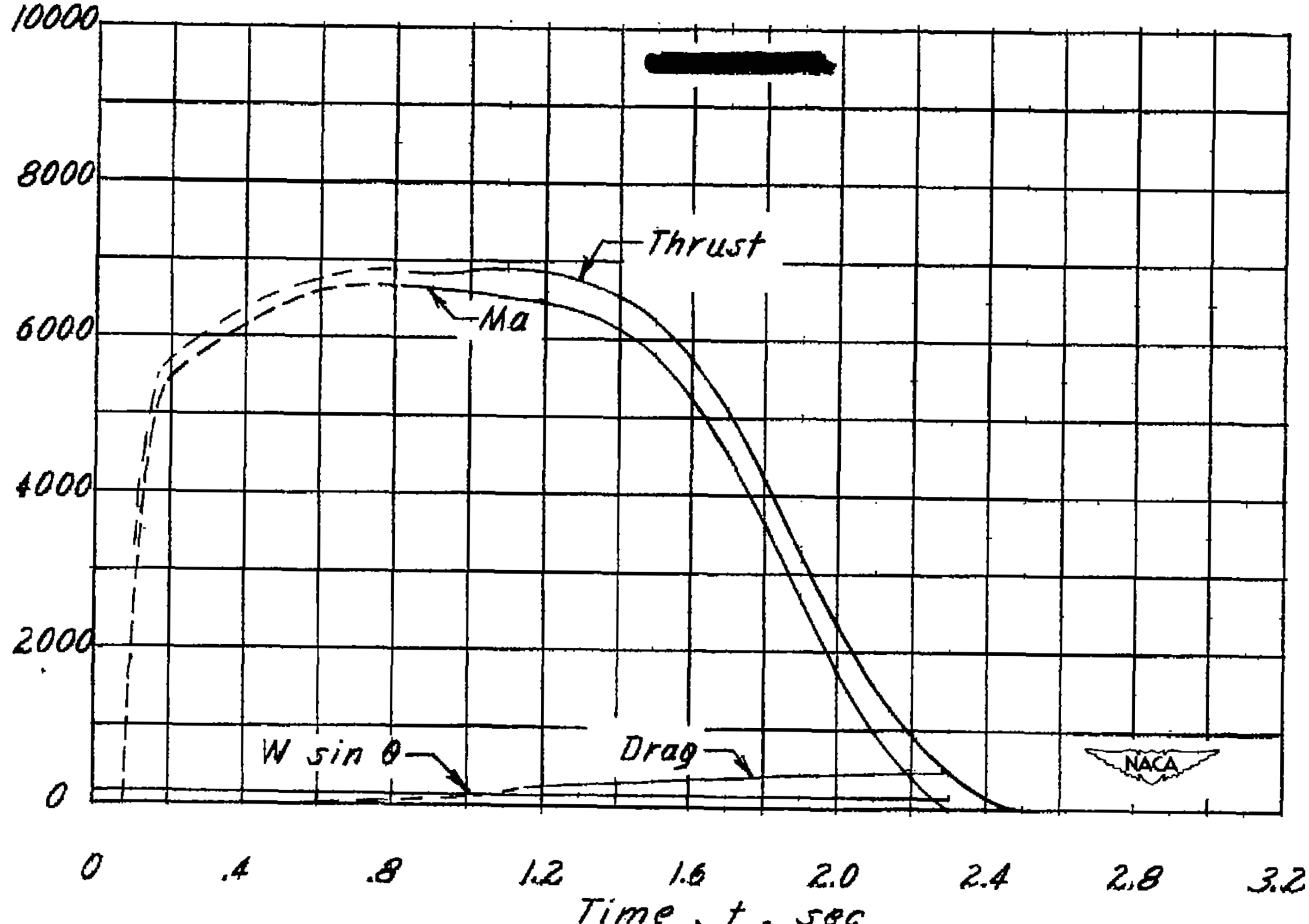

[redacted]

(i) Round 10.

Figure 5.- Concluded.

[redacted]

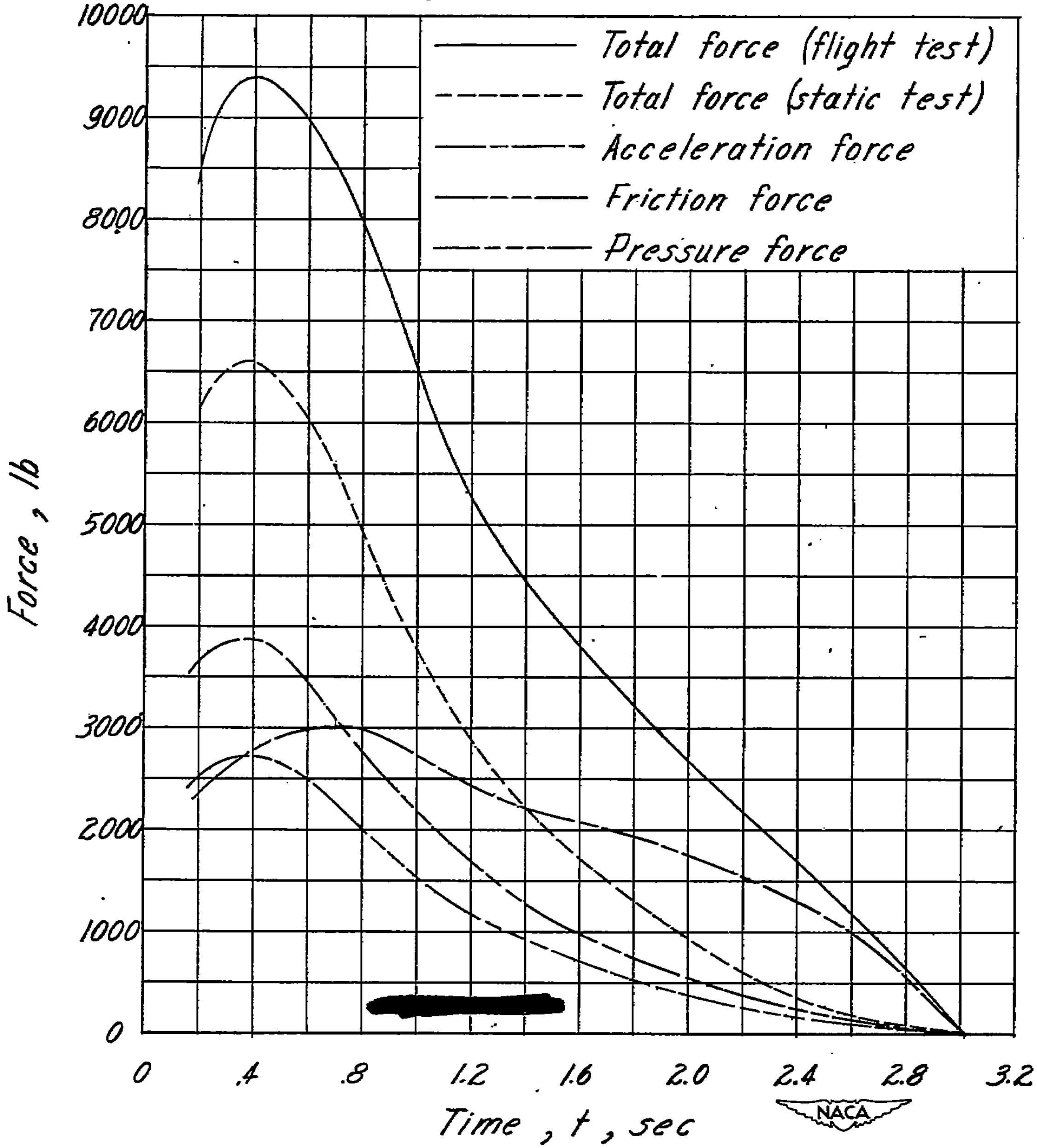

[redacted]

(a) Total force.

Figure 6.- Typical internal force-time history on grain of 6.25-inch Deacon rocket motor for round 5.

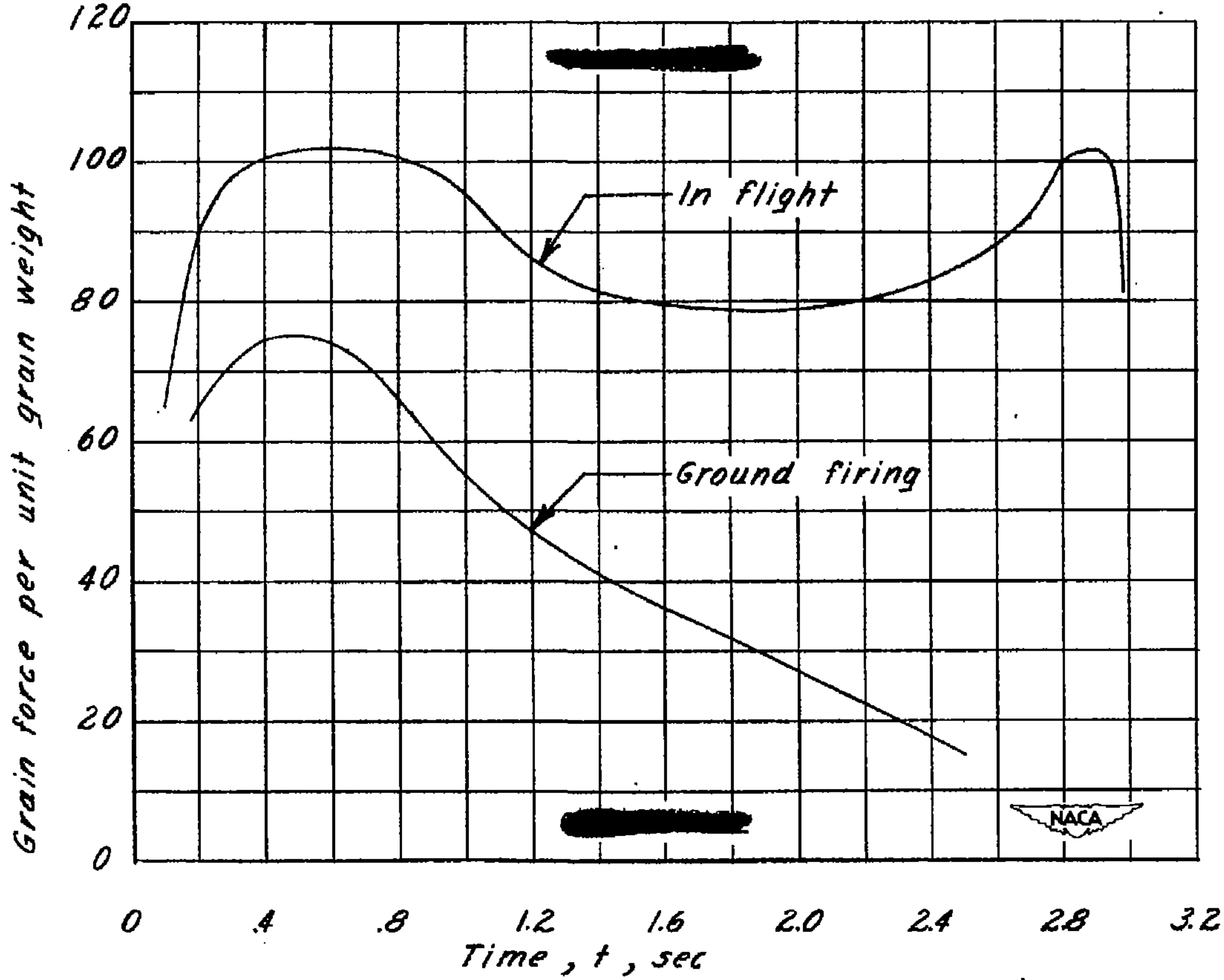

(b) Force per unit grain weight.
Figure 6.- Concluded.

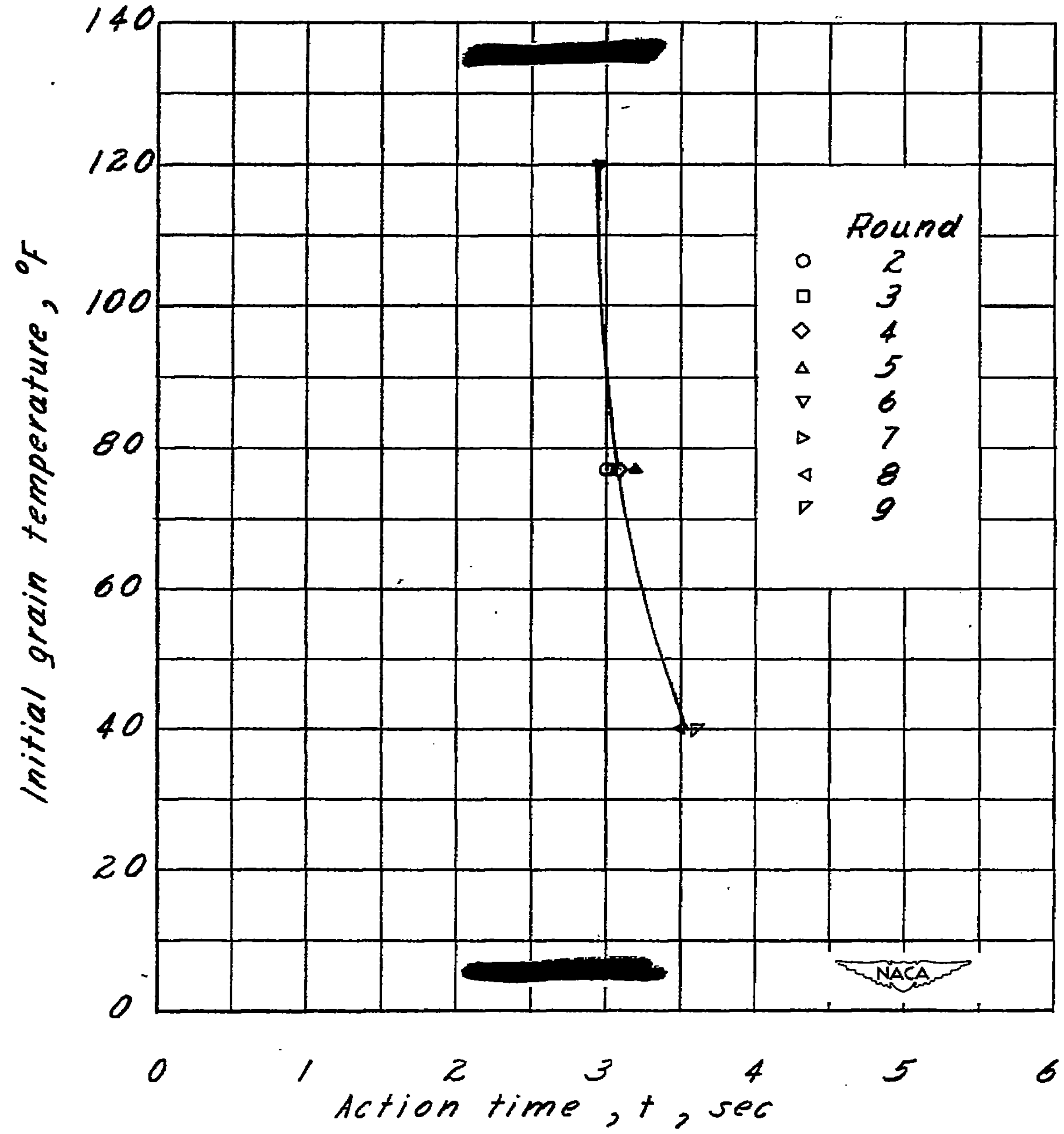

Figure 7.- Effect of initial grain temperature on action time of 6.25-inch Deacon rocket motor.

[redacted]

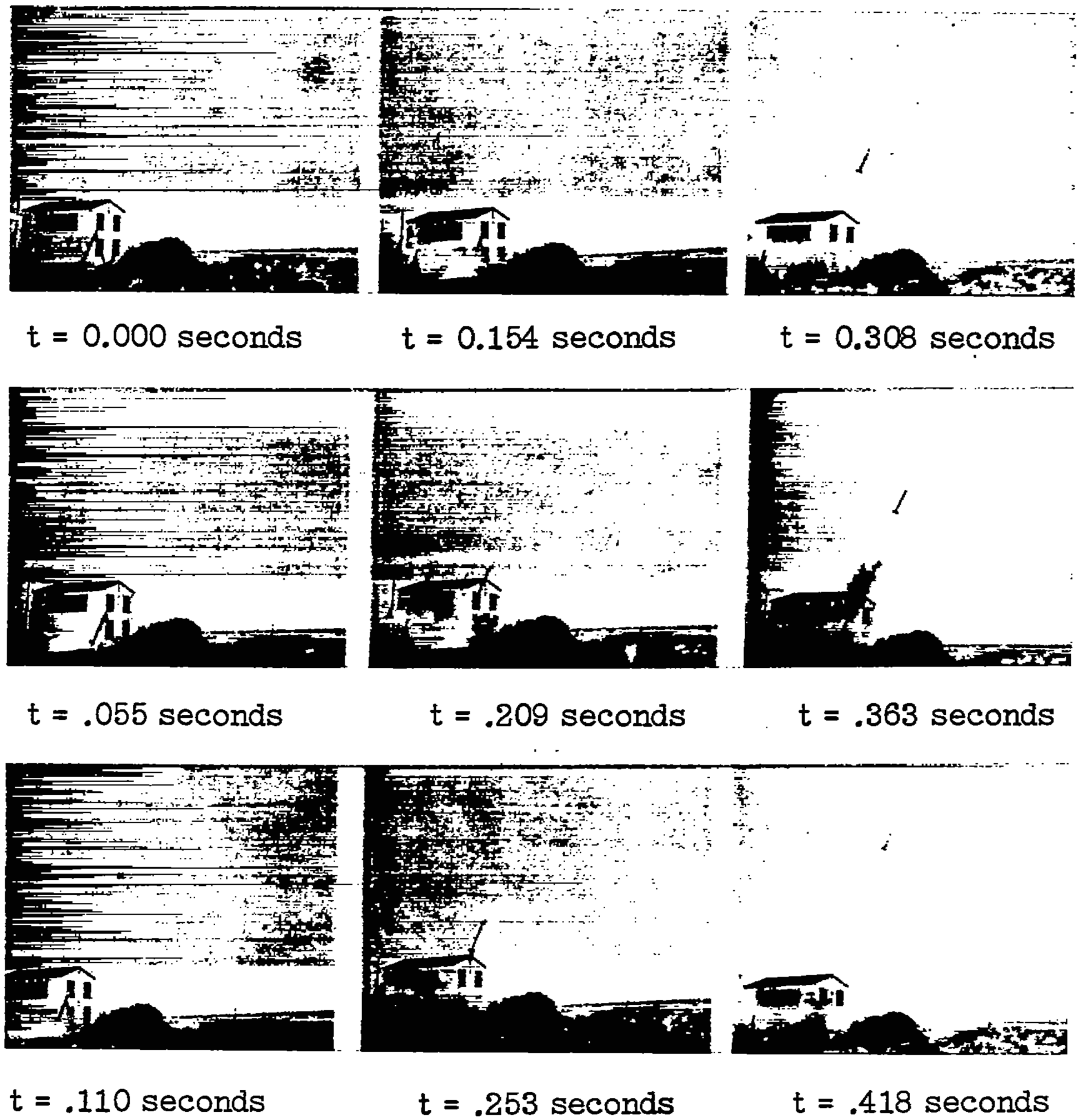

[redacted]

NACA
L-57208

Figure 8.- Selected photographs at take-off of 6.25-inch Deacon rocket motor. Round No. 1.

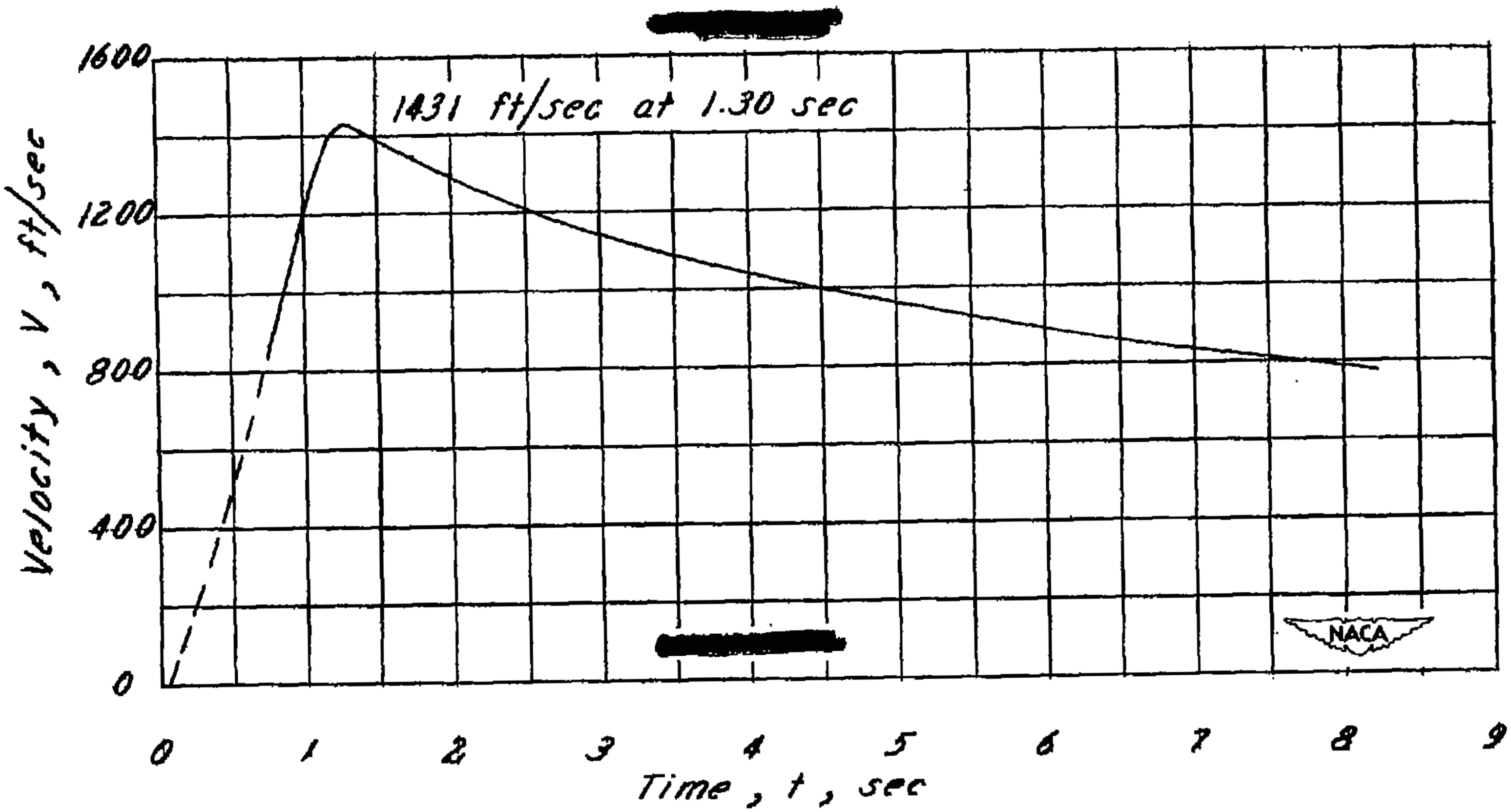

(a) Round 1.

Figure 9.- Velocity-time curves, 10-inch-scale model rocket motor.

[redacted]

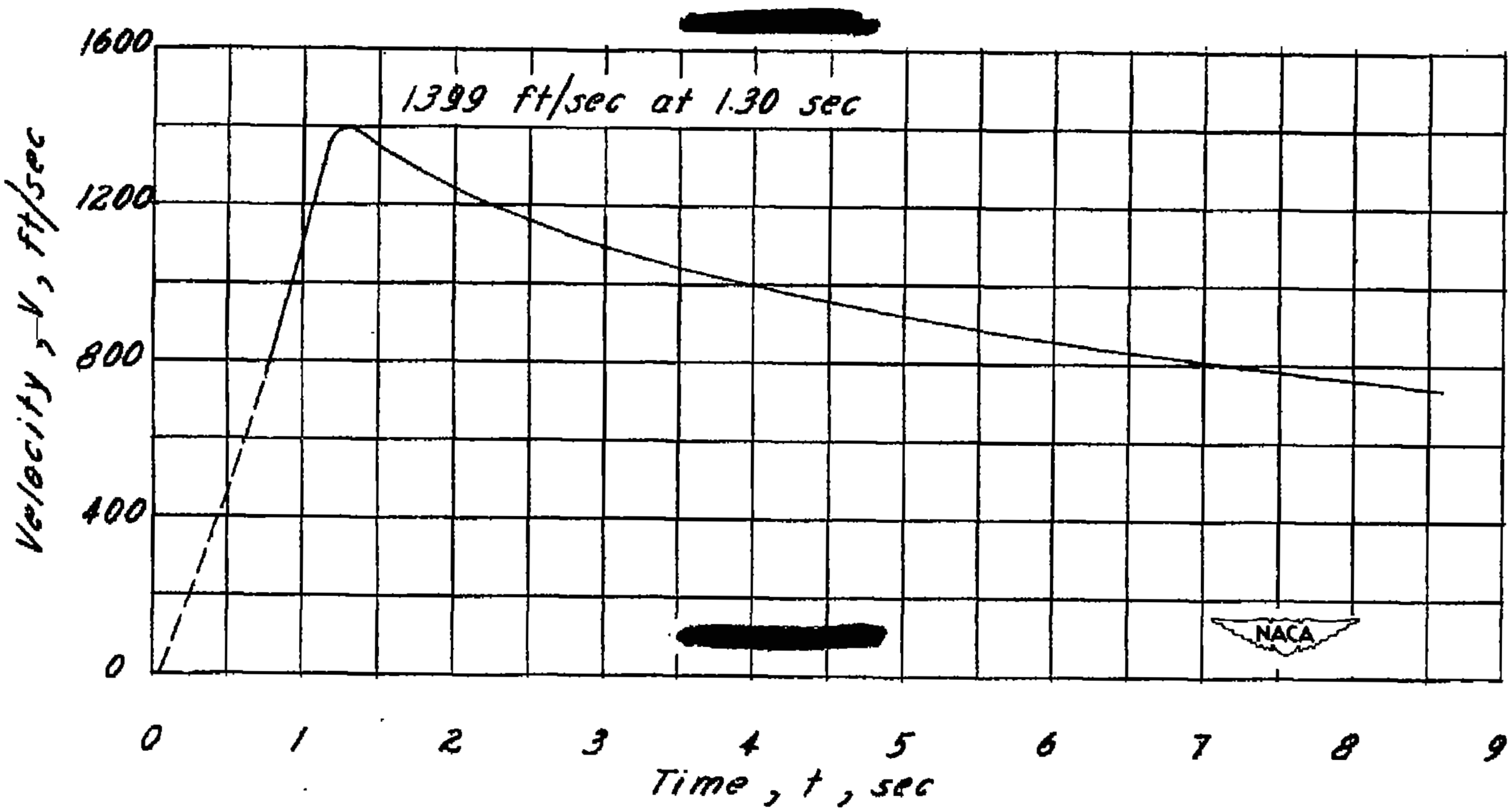

[redacted]

(b) Round 2.
Figure 9.- Continued.

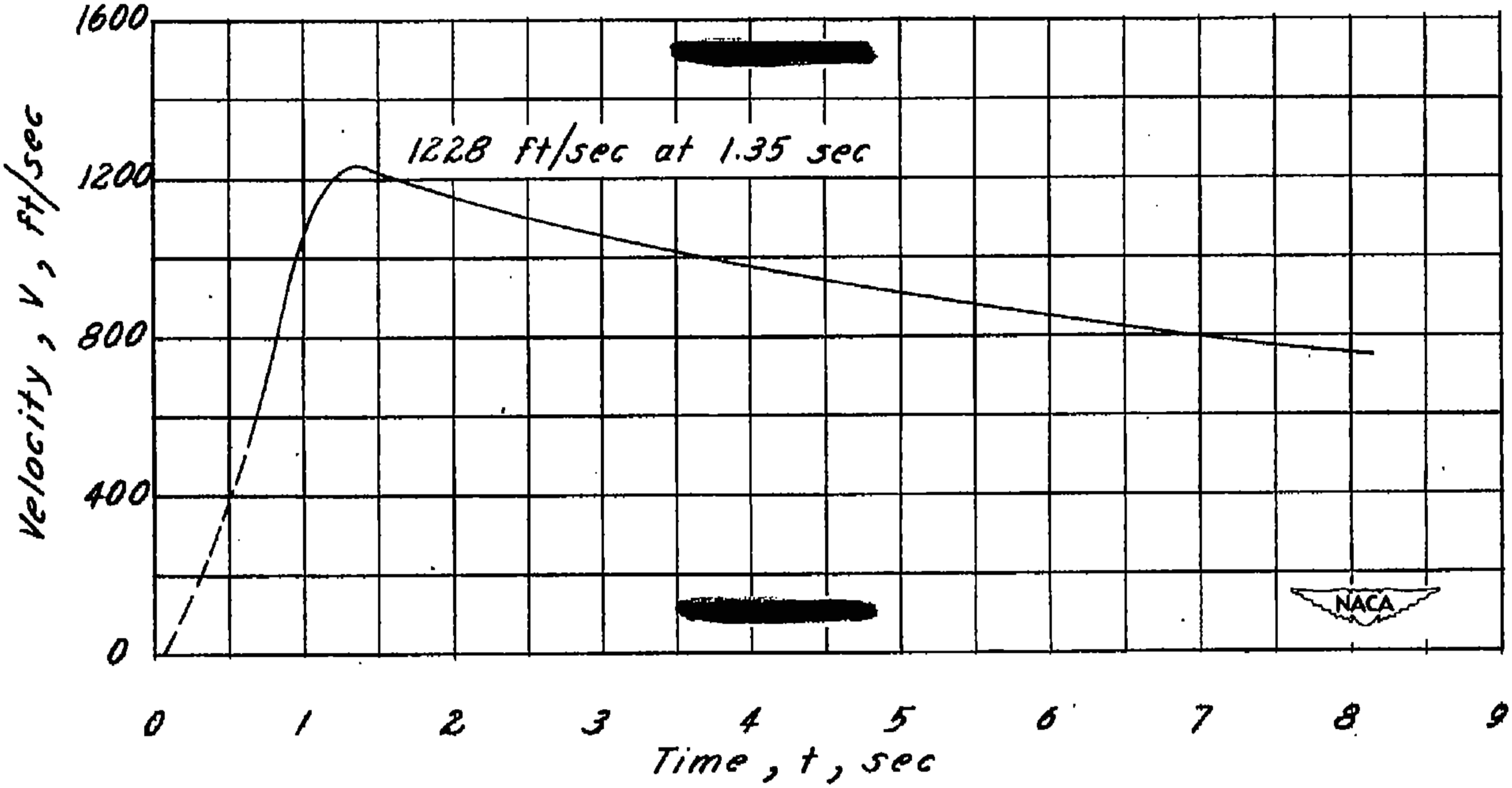

(c) Round 3.

Figure 9.- Continued.

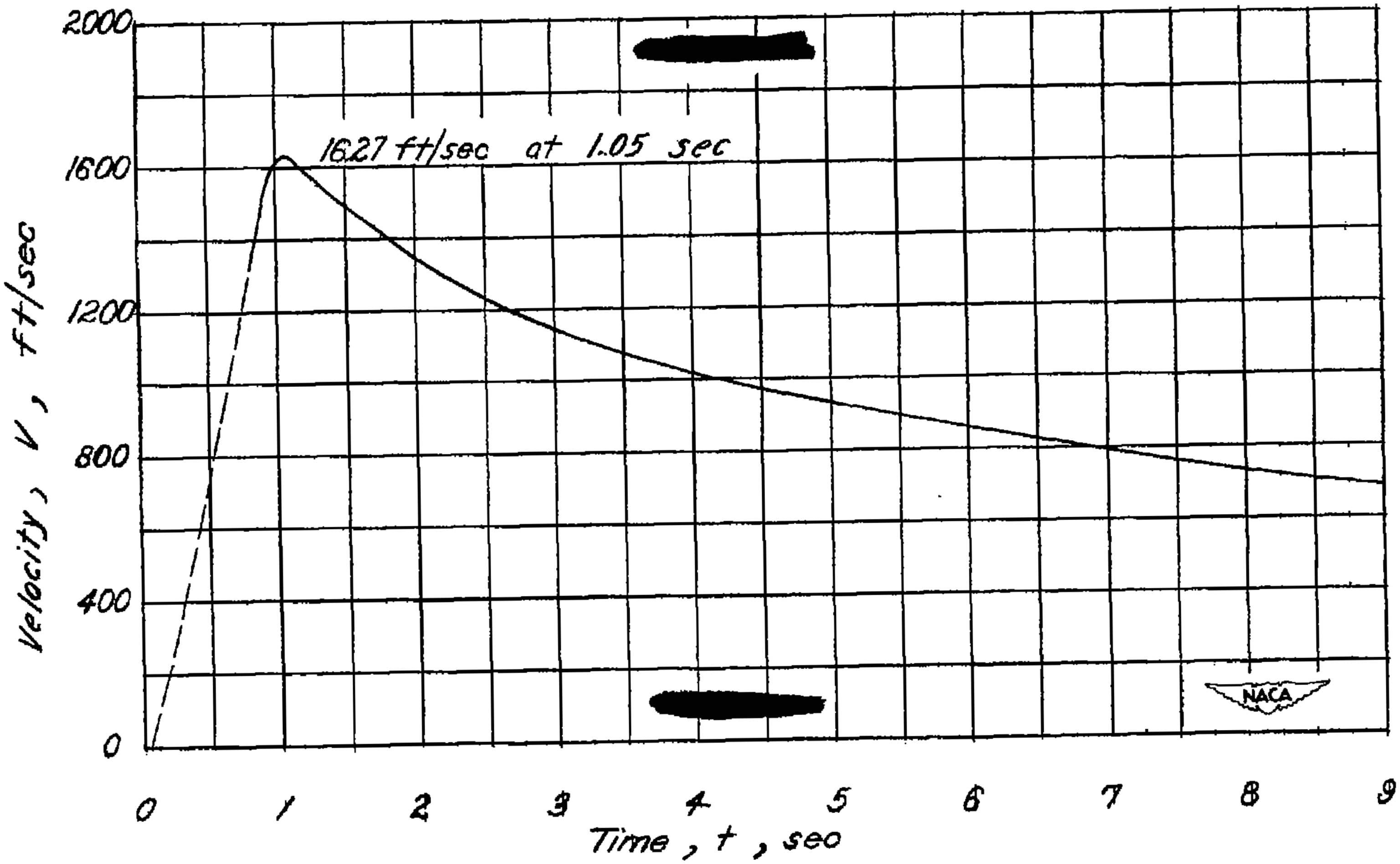

(d) Round 4.

Figure 9.- Continued.

[redacted]

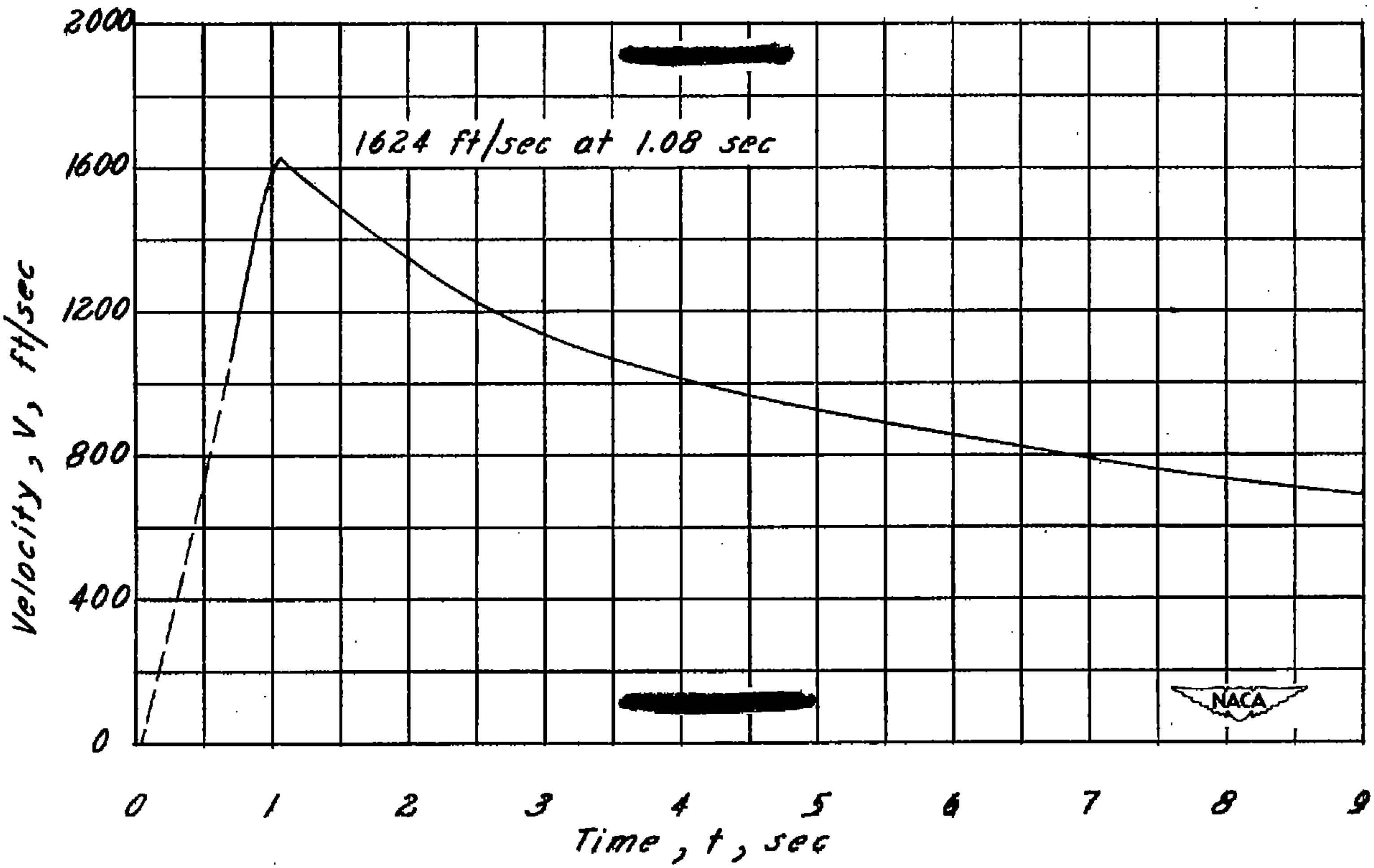

[redacted]

(e) Round 5.
Figure 9.- Continued.

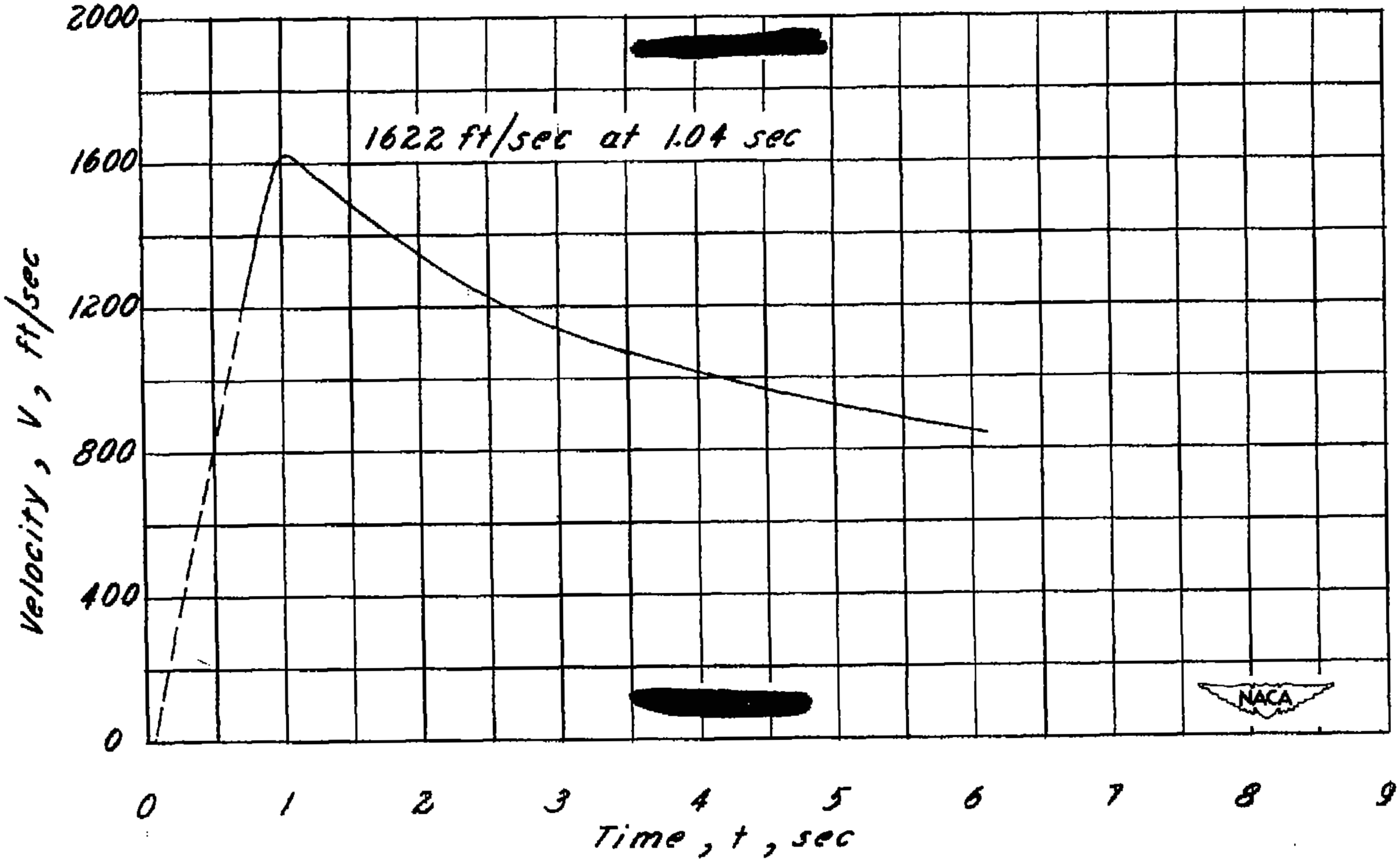

(f) Round 6.
Figure 9.- Continued.

[redacted]

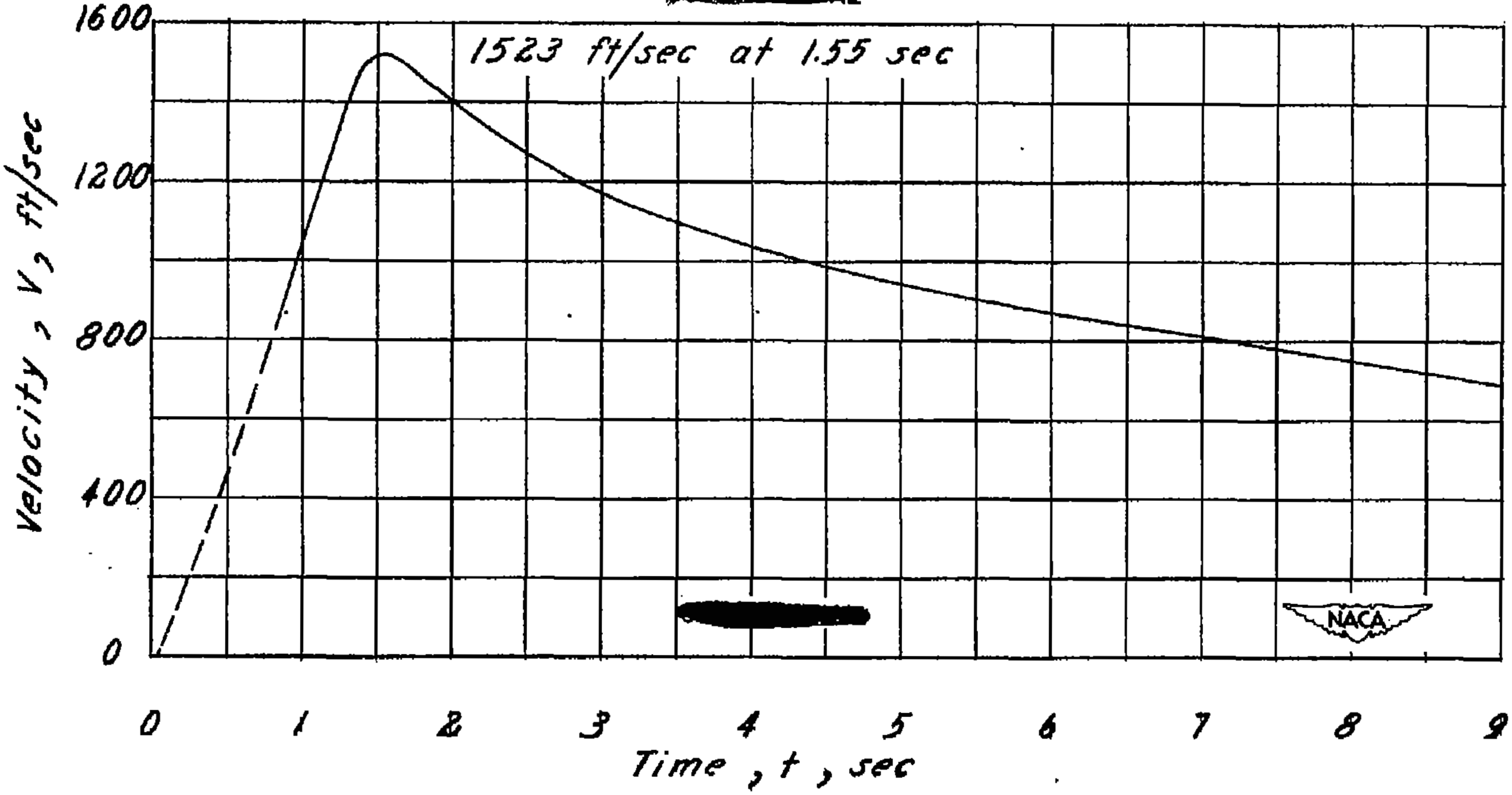

(g) Round 7.
Figure 9.- Continued.

[redacted]

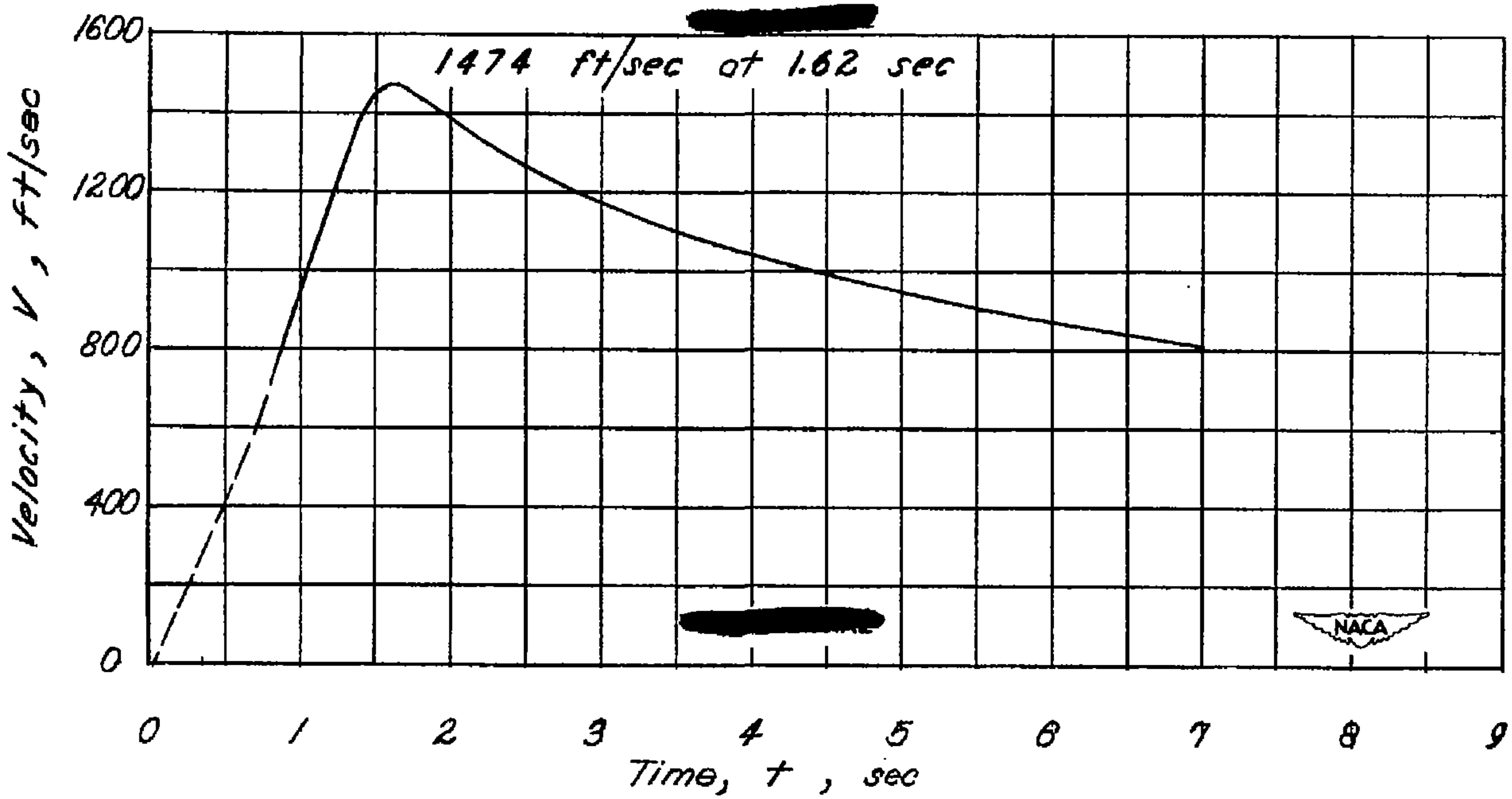

[redacted]

(h) Round 8.
Figure 9.—Concluded.

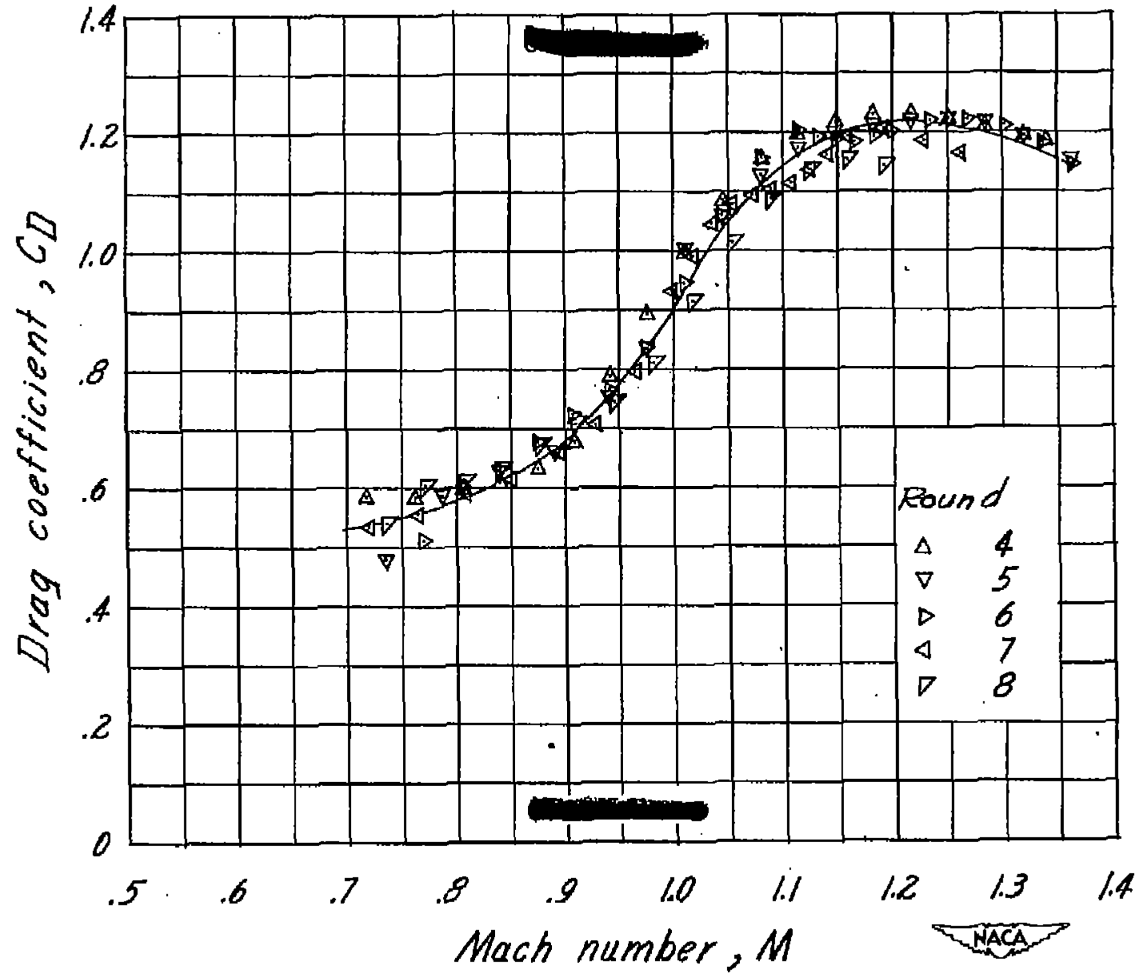

Figure 10.- Drag coefficient for 10-inch-scale model rocket motor.

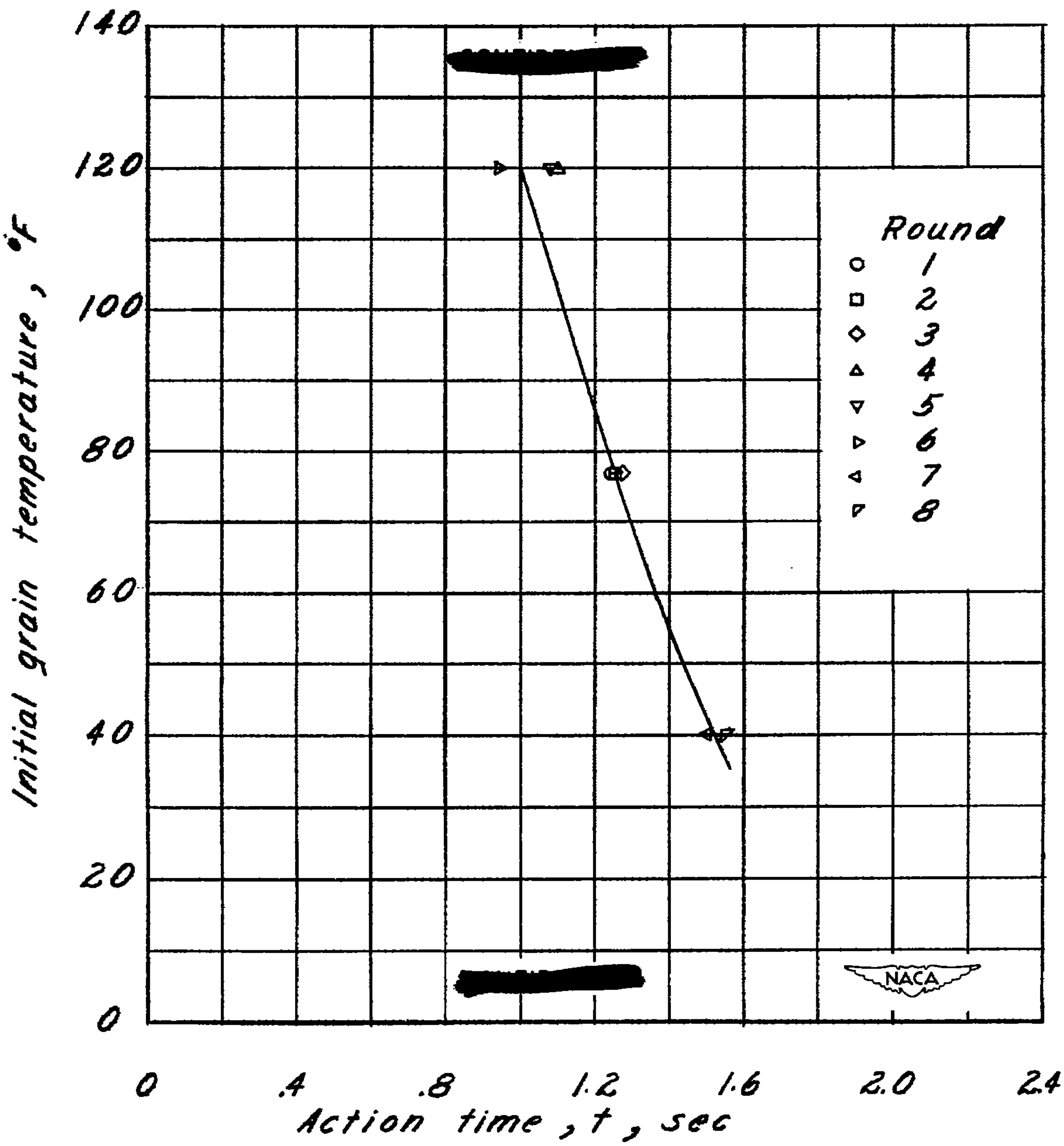

Figure 11.- Effect of initial grain temperature on action time of 10-inch-scale model rocket motor.